Title

Behavioral Timescale Cooperativity and Competitive Synaptic Interactions Regulate the Induction of Complex Spike Burst-Dependent Long-Term Potentiation.

Journal

Journal of Neuroscience, 42(13)

ISSN

0270-6474

Author

O'Dell, Thomas J

Publication Date

2022-03-30

DOI

10.1523/jneurosci.1950-21.2022

Peer reviewed

Cellular/Molecular

Behavioral Timescale Cooperativity and Competitive Synaptic Interactions Regulate the Induction of Complex Spike Burst-Dependent Long-Term Potentiation

Thomas J. O'Dell
Department of Physiology, David Geffen School of Medicine, and Integrative Center for Learning and Memory, Brain Research Institute, University of California Los Angeles, Los Angeles, California 90095

Although Hebbian LTP has an important role in memory formation, the properties of Hebbian LTP cannot fully account for, and in some cases seem incompatible with, fundamental properties of associative learning. Importantly, findings from computational and neurophysiological studies suggest that burst-dependent forms of plasticity, where dendritic spikes and bursts of action potentials provide the postsynaptic depolarization needed for LTP induction, may overcome some of the limitations of conventional Hebbian LTP. Thus, I investigated how excitatory synapses onto CA1 pyramidal cells interact during the induction of complex spike (CS) burst-dependent LTP in hippocampal slices from male mice. Consistent with previous findings, theta-frequency trains of synaptic stimulation induce a Hebbian form of plasticity where postsynaptic CS bursts provide the depolarization needed for NMDAR activation and LTP induction. However, in contrast to conventional Hebbian plasticity, where cooperative LTP induction requires coactivation of synapses on a timescale of tens of milliseconds, cooperative interactions between synapses activated several seconds apart can induce CS burst-dependent LTP. A novel, retroactive form of heterosynaptic plasticity, where activation of one group of synapses triggers LTP induction at other synapses that were active seconds earlier, also contributes to cooperativity in CS burst-dependent LTP. Moreover, competitive synaptic interactions that emerge during prolonged bouts of postsynaptic CS bursting potently regulate CS burst-dependent LTP. Together, the unusual properties of synaptic cooperativity and competition in CS burst-dependent LTP enable Hebbian synapses to operate and interact on behavioral timescales.

Key words: **complex spike burst; cooperativity; eligibility trace; LTP; synaptic competition**

Significance Statement

While EPSP-evoked complex spike (CS) bursting induces LTP at excitatory synapses onto hippocampal CA1 pyramidal cells, the properties of synaptic interactions during the induction of CS burst-dependent LTP have not been investigated. Here I report that interactions between independent synaptic inputs during the induction of CS burst-dependent LTP exhibit a number of novel, computationally relevant properties. Unlike conventional Hebbian LTP, the induction of CS burst-dependent LTP is regulated by proactive and retroactive cooperative interactions between synapses activated several seconds apart. Moreover, activity-dependent, competitive interactions between synapses allow strongly activated synapses to suppress LTP induction at more weakly activated synapses. Thus, CS burst-dependent LTP exhibits a number of the unique properties that overcome significant limitations of standard Hebbian plasticity rules.

Introduction

Coincident presynaptic and postsynaptic activity at excitatory synapses in many brain regions induces a long-lasting increase in synaptic strength, a phenomenon known as Hebbian LTP. Importantly, Hebbian LTP exhibits several properties, including rapid induction, long-term maintenance, and synapse specificity, that make it an attractive synaptic mechanism for memory formation (Dringenberg, 2020). Because of its dependence on activation of NMDA-type glutamate receptors (NMDARs), Hebbian LTP induction typically requires coactivation of multiple excitatory

Received Sep. 27, 2021; revised Dec. 27, 2021; accepted Jan. 31, 2022.

Author contributions: T.J.O. designed research; T.J.O. performed research; T.J.O. analyzed data; T.J.O. wrote the paper.

This work was supported by National Institute of Mental Health Grant 5R21MH115404-02. I thank Drs. Dean Buonomano, Seth Grant, and Peter Nguyen for helpful discussions during the course of this work and/or comments on the manuscript; and Ryan O'Dell for help with statistical analysis.

The author declares no competing financial interests.

Correspondence should be addressed to Thomas J. O'Dell at todell@mednet.ucla.edu.

https://doi.org/10.1523/JNEUROSCI.1950-21.2022

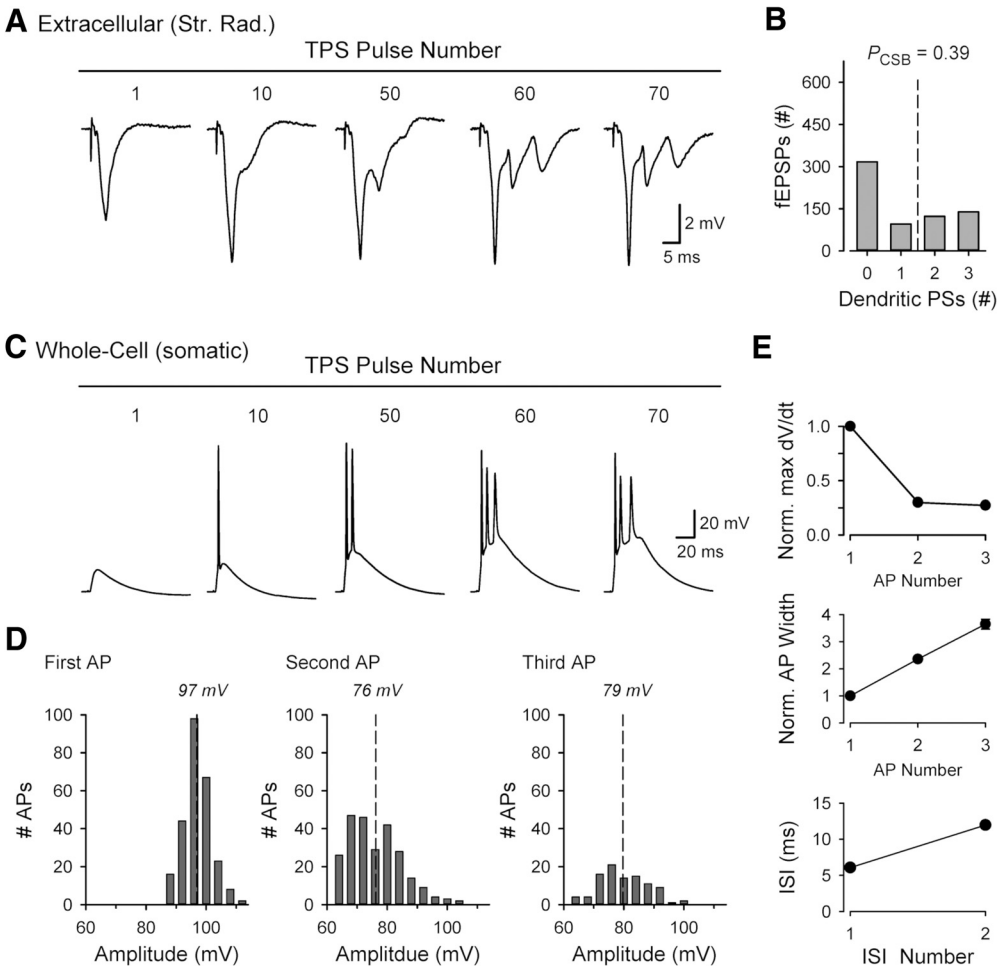

Figure 1. Theta-frequency stimulation-induced CS bursting. ***A***, Extracellular recording (in stratum radiatum) showing EPSP-evoked bursting during TPS. Note the negative-going PSs elicited by EPSPs during the train. ***B***, Histogram represents the number of EPSPs evoking 0-3 dendritic PSs and probably of EPSP-evoked CS bursts (P_{CSB}) during a 15 s train of TPS ($n = 9$ slices). ***C***, Somatic, whole-cell current-clamp recording showing EPSP-evoked CS bursting during TPS. ***D***, Histograms represent peak amplitudes for the first, second, and third APs in EPSP-evoked CS bursts ($n = 6$ cells). Dashed lines indicate mean AP amplitude. ***E***, Properties of CS burst APs. Plots represent maximum dV/dt during rising phase of each AP (top) and AP width at half-max (middle, both normalized to first AP). Bottom, Interspike intervals (ISI).

synaptic inputs to generate sufficient postsynaptic depolarization to relieve the voltage-dependent Mg^{2+} block of NMDAR channels, a property known as cooperativity (McNaughton et al., 1978; Lee, 1983). Cooperativity, in turn, enables LTP induction at synapses coactivated with stronger synaptic inputs (Barrionuevo and Brown, 1983; Kelso and Brown, 1986) or postsynaptic action potentials (APs) (Kelso et al., 1986; Sastry et al., 1986). Cooperativity thus provides a mechanism for associative interactions between synapses expected of a synaptic mechanism involved in associative learning (Kelso and Brown, 1986; Kelso et al., 1986).

Although LTP is thought to have an important role in associative forms of learning (Dringenberg, 2020), Hebbian plasticity alone cannot account for several fundamental properties of associative learning (Gallistel and Matzel, 2013). For example, because of the brief time course of NMDAR-mediated synaptic currents, there is a narrow time window lasting a few tens of milliseconds during which synapses can interact in an associative fashion to induce LTP (Gustafsson and Wigström, 1986; Kelso and Brown, 1986; Kelso et al., 1986; Debanne et al., 1996). In contrast, in Pavlovian conditioning, learning can occur when seconds or more separate conditional and unconditional stimuli. The cooperative synaptic interactions that underlie Hebbian LTP induction are also difficult to reconcile with phenomena, such as overshadowing (Pavlov, 1927; Mackintosh, 1976) and blocking (Kamin, 1969), which indicate an essential role for cue competition in regulating the allocation of associative strength to different cues during learning. Moreover, conventional Hebbian plasticity cannot account for the fact that associative forms of learning are dependent on predication errors; that is, robust learning occurs when conditional stimuli are paired with unpredicted or novel unconditional stimuli (for review, see Fanselow and Wassum, 2016).

Notably, modified versions of Hebbian plasticity rules can potentially overcome some of the limitations of conventional Hebbian LTP. For example, in neuromodulator-gated spike timing-dependent plasticity rules, coincident presynaptic and postsynaptic activity has no direct effect on synaptic strength but instead triggers biochemical changes that generate a synaptic eligibility trace that enables LTP induction in response to the delayed release of modulatory neurotransmitters (Izhikevich, 2007; Gerstner et al., 2018; Brzosko et al., 2019). Neuromodulator-gated spike timing-

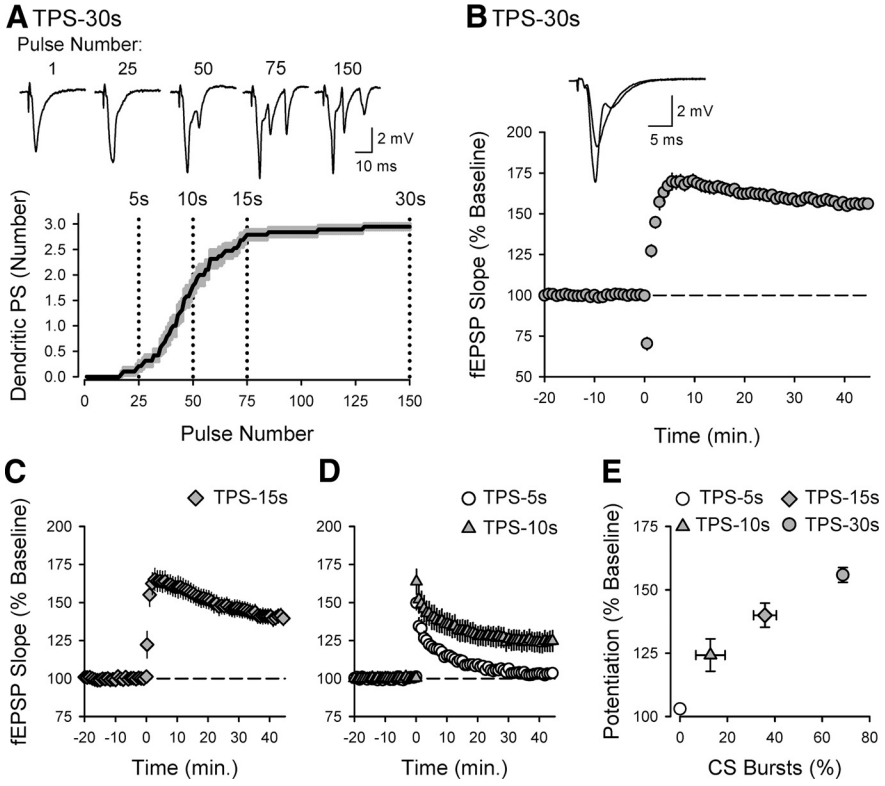

Figure 2. Activity dependence of TPS-induced CS bursting and LTP induction. ***A***, Plot represents number of dendritic PSs evoked by EPSPs during TPS (duration = 30 s). Shading represents ± SEM ($n = 19$). Traces represent fEPSPs evoked by the indicated pulse numbers during TPS. ***B***, LTP induction by a 30 s train of TPS (delivered at time = 0). At 45 min after TPS, fEPSPs were 156 ± 3% of baseline ($n = 19$). Traces represent superimposed fEPSPs recorded during baseline and 45 min after TPS. ***C***, 15 s of TPS was delivered at time = 0. At 45 min after TPS, fEPSPs were 140 ± 5% of baseline ($n = 18$). ***D***, At 45 min after TPS, fEPSPs were 124 ± 6% of baseline following 10 s of TPS ($n = 14$), and 103 ± 1% of baseline following 5 s of TPS ($n = 14$). TPS was delivered at time = 0. ***E***, Summary of results from experiments shown in ***B-D***. The magnitude of LTP induced by different TPS protocols is highly correlated with the amount of EPSP-evoked CS bursting (% of total TPS-evoked fEPSPs). Pearson product moment correlation: $r = 0.807$, $p = 5.05 \times 10^{-16}$, $n = 65$.

dependent plasticity rules thus enable Hebbian synapses to operate on behavioral timescales (because of the seconds-long persistence of eligibility traces) and potentiate in response to modulatory transmitters that provide information about prediction errors or novelty. Computational modeling suggests that another modified Hebbian plasticity rule, known as burst-dependent plasticity, can also overcome some of the limitations of conventional Hebbian LTP (Richards and Lillicrap, 2019; Magee and Grienberger, 2020; Payeur et al., 2021). In burst-dependent plasticity rules, feedback pathways that convey error signals synapse onto the apical dendrites of pyramidal neurons and provide an instructive signal that updates eligibility traces and potentiates synapses by triggering dendritic spikes and postsynaptic bursting. Although a burst-dependent form of plasticity known as behavioral timescale synaptic plasticity mediates the rapid formation of place fields in CA1 pyramidal cells (Bittner et al., 2017), the properties of burst-dependent LTP remain largely unexplored. Moreover, the role of cooperative and associative synaptic interactions in burst-dependent LTP has not been investigated.

Here, I investigated how excitatory synapses onto hippocampal CA1 pyramidal cells interact during the induction of a complex spike (CS) burst-dependent form of LTP. I find that CS burst-dependent LTP exhibits a number of remarkable properties, including an unusual form of cooperativity that operates on behavioral timescales, LTP induction mediated by CS burst-dependent updating of eligibility traces, and potent, activity-dependent competitive interactions between synapses.

Materials and Methods

Animals and slice preparation. Hippocampal slices from the dorsal third of the hippocampus were obtained from 2- to 3-month-old, male C57Bl/6 mice (Charles River Laboratories). Mice were deeply anesthetized with isoflurane and, following cervical dislocation, the brain was removed and place in cold (~4°C), oxygenated (95% O_2/5% CO_2) ACSF containing 124 mM NaCl, 4 mM KCl, 25 mM $NaHCO_3$, 1 mM NaH_2PO_4, 2 mM $CaCl_2$, 1.2 mM $MgSO_4$, and 10 mM glucose (all obtained from Sigma-Aldrich). Both hippocampi were then dissected from the brain, and a manual tissue slicer was used to prepare 400-μm-thick slices. The CA3 region was removed, and slices were then transferred to interface-type chambers continuously perfused with ACSF (2-3 ml/min) and allowed to recover (at 30°C) for at least 2 h before recordings. All techniques were approved by the Institutional Animal Care and Use Committee at the University of California, Los Angeles.

Electrophysiological recordings. Extracellular recordings were done using slices maintained in interface-type recording chambers perfused (2-3 ml/min) with ACSF. One or two bipolar, stimulating electrodes fabricated from twisted strands of Formvar-insulated nichrome wire (A-M Systems) were placed in stratum radiatum to activate Schaffer collateral/commissural fiber synapses onto CA1 pyramidal cells (basal stimulation rate = 0.02 Hz). Field EPSPs (fEPSPs) were recorded in stratum radiatum using low-resistance (5-10 MΩ) glass microelectrodes filled with ACSF and a Multi-clamp 700B amplifier (Molecular Devices). Signals were low pass filtered with a cutoff frequency of 2 kHz and digitized at 10 kHz. After determining the maximal amplitude of fEPSPs evoked by presynaptic fiber stimulation, the stimulation intensity was adjusted to evoke fEPSPs with an amplitude ~50% of the maximal amplitude. In experiments where two stimulating electrodes were used to activate independent Schaffer collateral fiber inputs onto CA1 pyramidal cells, one electrode was placed near the CA3 region and the other was placed on the opposite side of the recording electrode, near the subiculum. Independence of the presynaptic axons activated by the two stimulating electrodes (hereafter referred to as S1 and S2) was confirmed by the absence of paired-pulse facilitation when pulses of presynaptic fiber stimulation were delivered to S1 and then S2 (and vice-versa) with an interpulse interval of 50 ms. An approximately equal number of experiments were done using the stimulating electrode near the CA3 region or subiculum for S1 synapse stimulation and the designation of a particular stimulating electrode location as S1 or S2 had no effect on any of the findings reported here. Somatic, whole-cell current-clamp recordings were done using slices maintained in submerged-slice type recording chambers. In these experiments recording electrodes (resistance = 4-8 MΩ) were filled with a solution containing 122.5 mM K-gluconate, 17.5 mM KCl, 10 mM HEPES, 10 mM Na_2-phosphocreatine, 4 mM Mg-ATP, and 0.3 mM Na-GTP, pH 7.3. After allowing at least 3 min for whole-cell recordings to stabilize, the strength of

presynaptic fiber stimulation was adjusted to evoke ~15 mV EPSPs (basal stimulation rate = 0.05 Hz).

Experimental design and statistical analysis. CS burst-dependent LTP was induced using trains of theta-pulse stimulation (TPS) that consisted of single pulses of presynaptic fiber stimulation delivered at 5 Hz. In some experiments, LTP was also induced using a high-frequency stimulation (HFS) protocol consisting of two, 1-s-long trains of 100 Hz stimulation (intertrain interval [ITI] = 10 s). Average slopes of fEPSPs (normalized to baseline) recorded 40-45 min after TPS or 55-60 min after HFS were used for statistical comparisons. In extracellular recordings, EPSP-evoked CS bursting during TPS was quantified by visually inspecting fEPSPs evoked during TPS and counting the number of negative-going population spikes (PSs) elicited by individual EPSPs during the train. Population CS bursts were defined as fEPSPs containing 2 or more PSs and the probability of EPSP-evoked CS bursting (P_{CSB}), determined from the number of EPSPs eliciting CS bursts relative to total number of EPSPs evoked during TPS, was used for statistical comparisons. With extracellular recordings in stratum radiatum, the fEPSPs and PSs elicited during TPS both generate negative-going responses, making it difficult to measure PS amplitudes. Thus, in some experiments, a second recording electrode was placed in stratum pyramidale to record negative-going PSs occurring during the positive-going portion of the waveform generated by synaptic potentials. In these experiments, the amplitude of PSs evoked during TPS was measured as the average peak amplitude of the PS relative to the peak fEPSP amplitudes before and after each PS. The slope of the first fEPSP (recorded in stratum radiatum and normalized to baseline) elicited during a train of TPS delivered to S2 synapses was used to measure short-term heterosynaptic depression induced by a prior train of TPS delivered to S1 synapses. Paired and unpaired Student's *t* tests or, where appropriate, Mann–Whitney rank-sum tests were used to evaluate statistical significance between two groups. In cases where multiple comparisons were done, statistical significance was determined using one-way ANOVAs and Bonferroni *t* tests for *post hoc* comparisons or Kruskal–Wallis one-way ANOVAs on ranks with Dunn's *post hoc* tests. Data were collected and analyzed using pClamp10 software (Molecular Devices). Statistical tests were performed using SigmaPlot 12.5 (Systat Software). Values are reported as mean ± SEM, and full results of statistical tests are provided in the figure legends.

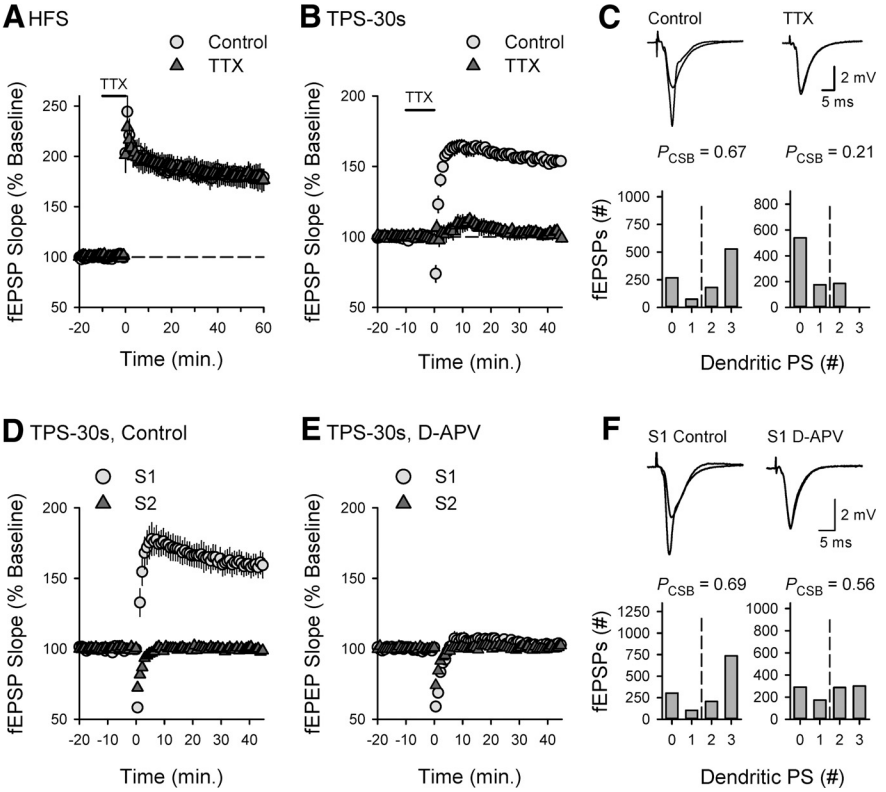

Figure 3. Postsynaptic CS bursting enables TPS-induced LTP. ***A***, HFS (delivered at time = 0) potentiated fEPSPs to 180 ± 6% of baseline in control experiments ($n = 6$) and 179 ± 11% of baseline in experiments where HFS was delivered in the presence of 0.2 μM TTX ($n = 5$, $t_{(9)} = 0.0934$, $p = 0.928$ compared with control). Bar represents TTX application. ***B***, At 45 min after TPS (duration = 30 s, delivered at time = 0), fEPSPs were potentiated to 154 ± 3% of baseline in control experiments ($n = 7$) and were 102 ± 3% of baseline in experiments where TPS was delivered in the presence of TTX ($n = 6$, $t_{(11)} = 12.685$, $p = 6.56 \times 10^{-8}$ compared with control). ***C***, Histograms represent the number of EPSPs evoking 0-3 dendritic PSs during TPS from all experiments. The probability of EPSP-evoked CS bursting (P_{CSB}) during TPS was significantly reduced when TPS was delivered in the presence of TTX (Mann–Whitney $U = 0$, $p = 0.001$). Traces represent superimposed fEPSPs recorded during baseline and 45 min after TPS in the presence (right) and absence of TTX (left). ***D***, Two stimulating electrodes were used to activate independent synaptic inputs, and TPS (duration = 30 s) was delivered to S1 synapses at time = 0. At 45 min after TPS, S1 fEPSPs were potentiated to 160 ± 8% of baseline and S2 fEPSPs were 99 ± 2% of baseline ($n = 9$). ***E***, TPS (duration = 30 s, delivered to S1 synapses at time = 0) had no lasting effect on synaptic transmission in slices continuously bathed in ACSF containing 50 μM D-APV. At 45 min after TPS, S1 fEPSPs were 102 ± 3% of baseline ($n = 7$, $t_{(14)} = 6.168$, $p = 2.44 \times 10^{-5}$ compared with control). Blocking NMDARs had no effect on the short-term heterosynaptic depression induced by S1 TPS (first S2 fEPSPs evoked following S1 TPS were 72 ± 2% and 74 ± 2% of baseline in control and D-APV experiments, respectively, $t_{(14)} = 0.595$, $p = 0.562$). ***F***, Histograms represent the number of EPSPs evoking 0-3 dendritic PSs during TPS from all experiments. P_{CSB} during TPS was significantly reduced when TPS was delivered in the presence of D-APV (Mann–Whitney $U = 8.5$, $p = 0.016$). Traces represent superimposed S1 fEPSPs recorded during baseline and 45 min after TPS in the presence (right) and absence of APV (left).

Results

EPSP-evoked CS bursting enables the induction of LTP by theta-frequency synaptic stimulation

TPS patterns of synaptic stimulation induce a striking facilitation of postsynaptic AP firing that leads to robust, EPSP-evoked bursting in CA1 pyramidal cells (Thomas et al., 1998; Winder et al., 1999; Brown et al., 2000; Tombaugh et al., 2002; Babiec et al., 2017). An example of this is shown in Figure 1*A* where, after ~50 pulses of TPS, fEPSPs recorded in stratum radiatum begin to elicit bursts of 2-3, negative-going PSs (Fig. 1*A*,*B*). The negative polarity of the EPSP-evoked PSs in stratum radiatum indicates that they are generated by current sinks located in the apical dendrites of CA1 pyramidal cells, perhaps because of back-propagating APs (Stuart and Sakmann, 1994; Magee and Johnston, 1997) and/or dendritic spikes that trigger somatic CS burst firing (Larkum et al., 1999; Magee and Carruth, 1999; Grienberger et al., 2014). Consistent with this notion, in experiments using somatic, whole-cell current-clamp recordings, EPSPs evoked during a 15-s-long train of TPS initially elicited single spikes but, as the train continued, began to elicit bursts containing 2-3 APs (Fig. 1*C*). Notably, the decrease in AP amplitudes (Fig. 1*D*) and rise times (Fig. 1*E*) as well as a progressive increase in AP duration and interspike intervals (Fig. 1*E*) during the EPSP-evoked bursts closely match the properties of APs generated during CS bursts recorded in CA1 pyramidal cells *in vivo*

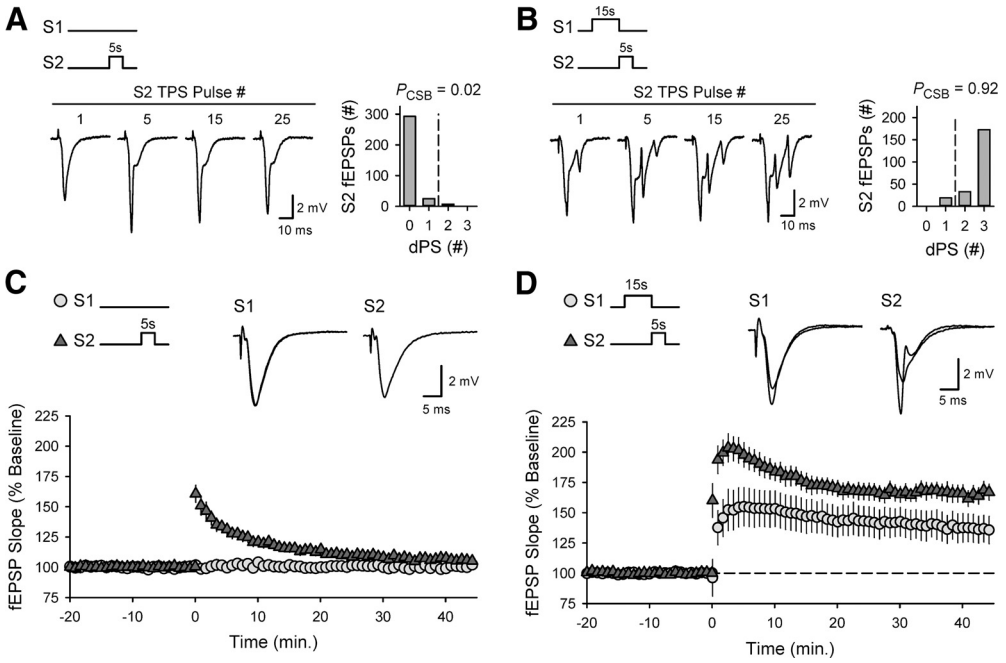

Figure 4. Heterosynaptic priming of EPSP-evoked CS bursting enables LTP induction by cooperative interactions between asynchronously activated synaptic inputs. ***A***, ***B***, Five seconds of TPS delivered to S2 synapses alone failed to elicit CS bursting (***A***) but induced robust CS bursting when delivered following a 15-s-long train of TPS delivered to S1 synapses (***B***). Traces represent fEPSPs elicited at the indicated stimulation pulse numbers during S2 TPS. Histograms represent the number of EPSPs eliciting 0-3 dendritic PSs during S2 TPS from all experiments. Although P_{CSB} was just 0.022 during a train of TPS delivered to S2 synapses alone ($n = 13$), P_{CSB} during S2 TPS was increased to 0.916 when S2 TPS was delivered after 15 s of TPS delivered to S1 synapses ($n = 9$) (Mann–Whitney $U = 1.0$, $p < 0.001$). ***C***, Five seconds of TPS delivered to S2 alone has no lasting effect on synaptic strength. At 45 min after TPS (delivered at time = 0), S2 fEPSPs were 106 ± 2% of baseline and S1 fEPSPs were 100 ± 1% of baseline ($n = 13$). ***D***, S2 synapses potentiate when S2 TPS (5 s) immediately follows 15 s of TPS delivered to S1 synapses. At 45 min after S1/S2 TPS (delivered at time = 0), S2 fEPSPs were potentiated to 165 ± 7% of baseline and S1 fEPSPs were 136 ± 11% of baseline ($n = 9$, $t_{(16)} = 2.160$, $p = 0.0463$). ***C***, ***D***, Superimposed fEPSPs recorded during baseline and 45 min after TPS.

(Epsztein et al., 2011; Grienberger et al., 2014). In addition, the preponderance of 2-3 spike bursts evoked during theta-frequency presynaptic stimulation is consistent with the activity dependence of CS bursting *in vivo* (Harris et al., 2001).

Although the underlying mechanisms are not well understood, EPSP-evoked CS bursting develops in a highly activity-dependent manner during theta-frequency patterns of synaptic stimulation. For example, EPSP-evoked CS bursting (defined as two or more negative-going PSs in stratum radiatum) is absent during the first 5 s of a 30-s-long train of TPS and CS bursts only begin to appear after ~7-10 s of TPS (Fig. 2*A*). Thereafter, the number of EPSP-evoked PSs continues to increase, and robust CS bursting (three EPSP-evoked PSs) develops by 15 s of TPS and then continues for the remainder of the stimulation train (Fig. 2*A*). Consistent with the notion that CS bursts provide the depolarization needed for NMDAR activation and LTP induction during TPS (Thomas et al., 1998), TPS trains lasting ≥15 s induced robust LTP (Fig. 2*B*,*C*). In contrast, trains that ended soon after the onset of CS bursting (10 s duration) or terminated before EPSP-evoked CS bursting begins (5 s duration) induced modest or no LTP (Fig. 2*D*). Thus, the magnitude of LTP induced by different duration trains of TPS is highly correlated with the amount of EPSP-evoked CS bursting (Fig. 2*E*).

To confirm that CS bursting is indeed required for TPS-induced LTP, I next compared the effects of inhibiting burst firing in CA1 pyramidal cells with a low concentration of TTX (Azouz et al., 1996; Thomas et al., 1998; Magee and Carruth, 1999) on the induction of LTP by TPS and HFS protocols. Although a 10 min bath application of 0.2 μM TTX had no effect on HFS-induced LTP (Fig. 3*A*), it significantly reduced EPSP-evoked CS bursting and prevented the induction of LTP by 30 s of TPS (Fig. 3*B*,*C*). These results, along with those shown in Figure 2, indicate that TPS induces a CS burst-dependent form of LTP. Consistent with the notion that EPSP-evoked CS bursting induces an NMDAR-dependent form of LTP, the potentiation induced by 30 s of TPS was both synapse-specific (Fig. 3*D*) and inhibited by the NMDAR antagonist D-APV (Fig. 3*E*). Blocking NMDARs also produced a small, but significant ($p < 0.02$), inhibition of EPSP-evoked CS bursting during TPS (Fig. 3*F*), suggesting that NMDAR-mediated synaptic potentials contribute to CS burst firing during TPS (see Grienberger et al., 2014; Babiec et al., 2017). APV had no effect, however, on the short-term heterosynaptic depression of S2 synapses induced by 30 s of TPS delivered to S1 synapses (Fig. 3*D*,*E*).

Heterosynaptic priming of EPSP-evoked CS bursting generates a novel form of cooperative LTP induction

The TPS-induced switch in the mode of AP generation from single spiking to burst firing (Figs. 1 and 2*A*) could arise from highly localized, synapse-specific increases in EPSP-spike coupling (Fink and O'Dell, 2009). However, CS bursting in pyramidal neurons is produced by dendritic spikes generated by activation of voltage-gated Ca^{2+} channels and/or NMDARs (Magee and Carruth, 1999; Takahashi and Magee, 2009; Grienberger et al., 2014). Moreover, GABAergic inhibition, which is downregulated by theta-frequency patterns of synaptic activity (Davies et al., 1991; Mott and Lewis, 1991; Klyachko and Stevens, 2006; Babiec et al., 2017), potently suppresses burst firing in pyramidal neurons (Larkum et al., 1999; Lovett-Barron et al., 2012; Royer et al., 2012). Thus, the emergence of CS bursting

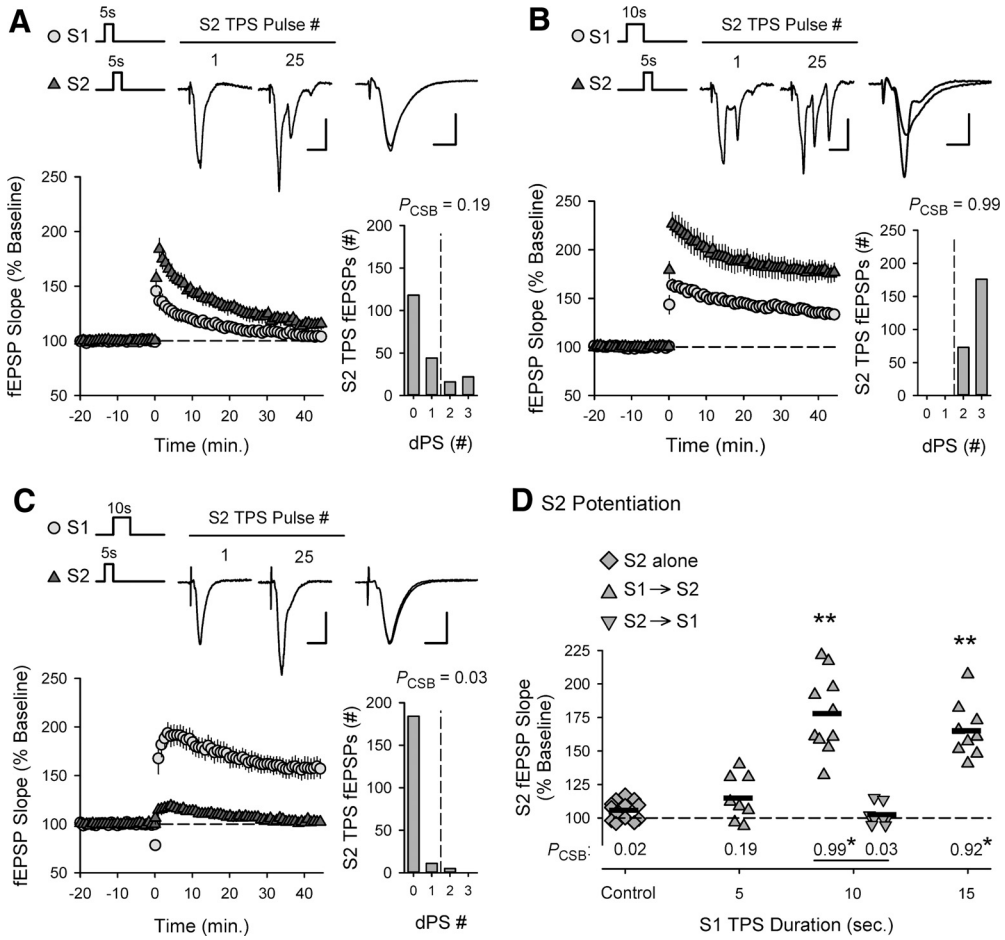

Figure 5. Activity- and pattern-dependent regulation of cooperativity in CS burst-dependent LTP. ***A***, Five seconds of TPS delivered to S2 synapses had little lasting effect on synaptic transmission when S2 TPS follows a 5 s train of TPS delivered to S1 synapses ($n = 8$). ***B***, Five seconds of S2 TPS delivered after a 10 s train of TPS delivered to S1 TPS induced robust LTP at S2 synapses ($n = 10$). ***C***, S2 synapses were not potentiated when the pattern of S1/S2 TPS was reversed (5 s of S2 TPS delivered before 10 s of S1 TPS, $n = 8$). ***A-C***, Histograms represent number of EPSPs that elicit 0-3 dendritic PSs during S2 TPS from all experiments. ***A-C***, Traces represent the first and last fEPSPs elicited during S2 TPS train (left; calibration: 2.0 mV, 10 ms) and superimposed S2 fEPSPs recorded during baseline and 45 min after S2 TPS (right; calibration: 2.0 mV, 5.0 ms). ***D***, Symbols represent change in S2 fEPSP slopes (45 min after S1/S2 TPS) from all individual experiments. Plot includes results from experiments shown in Figure 4*C*, *D*. Bars indicate mean values. $^{**}p < 0.001$, compared with control, one-way ANOVA with Bonferroni *t* test *post hoc* comparisons ($F_{(6,55)} = 33.191$, $p < 0.001$). Numbers indicate P_{CSB} during S2 TPS. $^{*}p < 0.05$, compared with control, one-way ANOVA on ranks with Dunn's test *post hoc* comparisons ($H_{(4)} = 40.375$, $p < 0.001$).

during TPS might arise from more widespread, postsynaptic changes in dendritic excitability and/or a decrease in feedforward inhibition.

To determine whether the induction of EPSP-evoked CS bursting by TPS is because of synapse-specific changes in EPSP/spike coupling or instead involves increases in pyramidal cell excitability, two stimulating electrodes (S1 and S2) were placed in stratum radiatum to activate independent groups of Schaffer collateral synapses. Two sequential, nonoverlapping trains of TPS were then delivered to determine whether the prior induction of EPSP-evoked CS bursting by a long train of TPS (15 s duration) at S1 synapses alters the mode of AP firing elicited by EPSPs evoked during a brief train of TPS (5 s duration) at S2 synapses (Fig. 4). In control experiments, 5 s of TPS delivered to S2 synapses alone elicited few CS bursts ($P_{CSB} = 0.022$, $n = 13$) (Fig. 4*A*) and had no lasting effect on synaptic strength (45 min after TPS S2 fEPSPs were 106 ± 2% of baseline) (Fig. 4*C*). EPSP-evoked CS bursting was dramatically enhanced at S2 synapses, however, when TPS delivered to S2 synapses followed 15 s of TPS delivered to S1 synapses ($P_{CSB} = 0.916$, $n = 9$) (Fig. 4*B*) and S2 fEPSPs potentiated to 165 ± 7% of baseline (Fig. 4*D*). Notably, the potentiation of S2 synapses exceeded that induced at S1 synapses, although far fewer stimulation pulses were delivered to S2 synapses (Fig. 4*D*). The heterosynaptic facilitation of EPSP-evoked CS busting at S2 synapses produced by S1 TPS indicates that the induction of EPSP-evoked CS bursting is not synapse-specific. Instead, TPS induces more widespread changes in pyramidal cell excitability that enable independent, asynchronously activated synapses to interact in a highly cooperative fashion to elicit postsynaptic CS bursts and undergo LTP. The TPS protocol used for the experiments shown in Figure 4*D* had no lasting effect on synaptic strength at S2 (or S1) synapses when TPS trains were delivered in the presence of the NMDAR antagonist D-APV (50 μM, $n = 7$; data not shown). Thus, the heterosynaptic facilitation of EPSP-evoked CS bursting induced by TPS delivered to S1 synapses enables the induction of NMDAR-dependent LTP at S2 synapses.

The heterosynaptic facilitation of CS bursting and LTP induction by 5 s of TPS delivered to S2 synapses was highly dependent

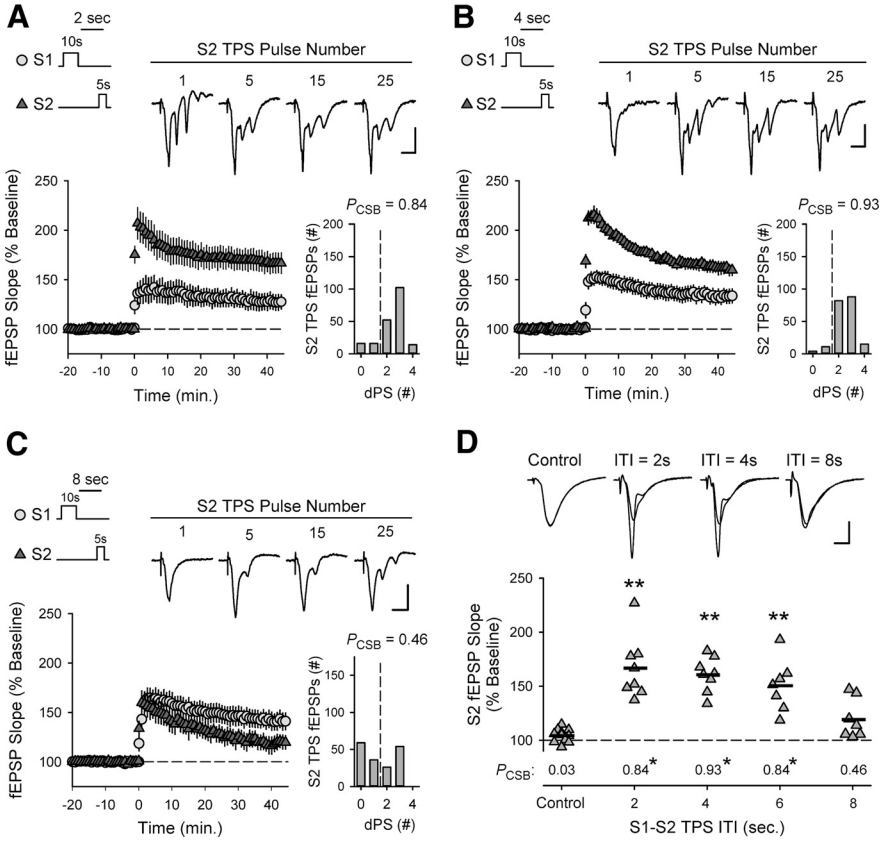

Figure 6. CS burst-dependent LTP exhibits behavioral timescale cooperativity. ***A-C***, TPS (5 s) was delivered to S2 synapses 2 (***A***, $n = 8$), 4 (***B***, $n = 8$), or 8 s (***C***, $n = 7$) after a 10-s-long train of TPS delivered to S1 synapses. Traces represent S2 fEPSPs evoked by the indicated pulse number during TPS. Calibration bars: 2.0 mV, 10.0 ms. Histograms represent number of fEPSPs that elicited 0-4 dendritic PSs during S2 TPS from all experiments. ***D***, Summary plot showing results from all experiments. Symbols represent change in S2 fEPSP slopes (45 min after TPS) from individual experiments. Bars indicate mean values. $^{**}p < 0.001$, compared with interleaved control experiments (5 s of TPS delivered to S2 alone, $n = 11$), one-way ANOVA with Bonferroni *t* test *post hoc* comparisons ($F_{(5,42)} = 21.163$, $p < 0.001$). Numbers indicate P_{CSB} during S2 TPS. $^{*}p < 0.05$, compared with control, one-way ANOVA on ranks with Dunn's test *post hoc* comparisons ($H_{(4)} = 26.777$, $p < 0.001$). The magnitude of LTP induced at S2 synapses was significantly correlated with the P_{CSB} during S2 TPS (Pearson product moment correlation: $r = 0.758$, $p = 9.27 \times 10^{-9}$, $n = 41$). Traces represent superimposed S2 fEPSPs recorded during baseline and 45 min after S2 TPS from a control experiment (S2 TPS alone) and in experiments with different S1 → S2 TPS ITIs. Calibration: 2.0 mV, 5 ms.

on the duration of TPS delivered to S1 synapses (Fig. 5). For example, a brief train of S1 TPS (5 s) that was below threshold for the induction of CS bursting had little effect on the ability of a subsequent train of TPS delivered to S2 synapses to evoke CS bursts and induce LTP (Fig. 5*A*). Increasing the duration of TPS delivered to S1 synapses to 10 s, however, strongly facilitated both TPS-induced CS bursting and LTP at S2 synapses (Fig. 5*B*). Thus, the ability of TPS trains delivered to S1 synapses to facilitate LTP induction at S2 synapses closely matches the activity dependence of TPS-induced bursting (Fig. 2*A*). This suggests that the heterosynaptic facilitation of EPSP-evoked CS bursting mediates cooperative synaptic interactions in TPS-induced LTP. Indeed, although 10 s of S1 TPS delivered before S2 TPS strongly facilitated EPSP-evoked CS bursting and LTP induction at S2 synapses (Fig. 5*B*), S2 synapses did not undergo LTP when TPS was delivered to S2 synapses before the induction of CS bursting by a 10-s-long train of TPS delivered to S1 synapses (Fig. 5*C*). Moreover, for the experiments shown in Figures 4 and 5, the magnitude of LTP induced by 5 s of TPS delivered to S2 synapses was highly correlated with the probability of EPSP-evoked CS bursting during S2 TPS (Pearson product moment correlation: $r = 0.854$, $p = 1.14 \times 10^{-14}$, $n = 48$).

CS burst-dependent LTP exhibits behavioral timescale cooperativity

The ability of synapses activated by HFS protocols to act in a cooperative manner to induce Hebbian LTP requires near synchronous coactivation of synaptic inputs onto CA1 pyramidal cells (Gustafsson and Wigström, 1986; Kelso and Brown, 1986; Kelso et al., 1986; Debanne et al., 1996). Thus, the cooperative induction of CS burst-dependent LTP by asynchronous activation of independent synapses is unusual and raises a number of intriguing questions. For example, does the CS burst mode of AP firing induced during TPS persist after the stimulation train and, if so, does cooperativity in CS burst-dependent LTP operate over longer timescales compared with conventional Hebbian LTP?

Because the timescale of the cooperativity between different synapses is of fundamental computational importance, I next examined how the heterosynaptic facilitation of TPS-induced LTP is altered when a delay is introduced between trains of TPS delivered to S1 and S2 synapses. In these experiments, 10 s of TPS was delivered to S1 synapses to induce EPSP-evoked CS bursting and a 5-s-long train of TPS was then delivered to S2 synapses with ITIs ranging from 2 to 8 s (Fig. 6). In interleaved control experiments, where 5 s of TPS was delivered to S2 synapses alone, few EPSPs evoked during TPS elicited CS bursts ($P_{CSB} = 0.029$) and 45 min after TPS fEPSPs evoked at S2 synapses were $104 \pm 2\%$ of baseline ($n = 11$). In contrast, EPSP-evoked CS bursting during S2 TPS was strongly enhanced ($P_{CSB} = 0.84$) and S2 fEPSPs potentiated to $167 \pm 10\%$ of baseline ($n = 8$) when S2 TPS was delivered 2 s after S1 TPS (Fig. 6*A*). CS bursting during S2 TPS was also significantly facilitated and S2 synapses potentiated when trains of S2 TPS were delivered 4 (Fig. 6*B*) or 6 s after S1 TPS (Fig. 6*D*). However, when the S1-S2 TPS ITI was increased to 8 s, the amount of EPSP-evoked CS bursting during S2 TPS was reduced and the potentiation of S2 synapses was not significantly different from that seen in control experiments (Fig. 6*C*,*D*). Together, these results indicate that the CS burst mode of AP firing induced by TPS persists for several seconds after the stimulation train, and thus generates a strikingly long window spanning at least 6 s during which synapses can interact in a cooperative fashion to induce LTP.

Activity-dependent, competitive interactions between synapses inhibit cooperativity in CS burst-dependent LTP

To better define the activity dependence of cooperativity in CS burst-dependent LTP, I next examined whether conditioning trains of S1 TPS lasting longer than 15 s, which induce more

robust postsynaptic CS bursting (Fig. 2*A*) and homosynaptic LTP (Fig. 2*D*), produce a stronger heterosynaptic facilitation of LTP induction at S2 synapses. In control experiments, 10 s of TPS delivered to S1 synapses induced a modest potentiation at S1 synapses (45 min after TPS fEPSPs were 129 ± 4% of baseline, $n = 8$) but strongly facilitated the induction of LTP by a 5-s-long train of TPS delivered to S2 synapses (S2 synapses potentiated to 173 ± 7% of baseline) (Fig. 7*A*). Surprisingly, although increasing the duration of TPS delivered to S1 synapses to 20 or 25 s induced larger homosynaptic LTP at S1 synapses (S1 fEPSPs were potentiated to 156 ± 8% [$n = 7$] and 170 ± 6% [$n = 13$] of baseline, respectively), the heterosynaptic facilitation of LTP induction at S2 synapses was abolished (Fig. 7*B–D*). Thus, heterosynaptic facilitation of LTP induction at S2 synapses exhibits a pronounced, inverted U-shaped dependence on the duration of TPS trains delivered to S1 synapses (Fig. 7*E*), suggesting that longer duration trains of TPS induce a form of synaptic competition that strongly inhibits cooperativity in CS burst-dependent LTP.

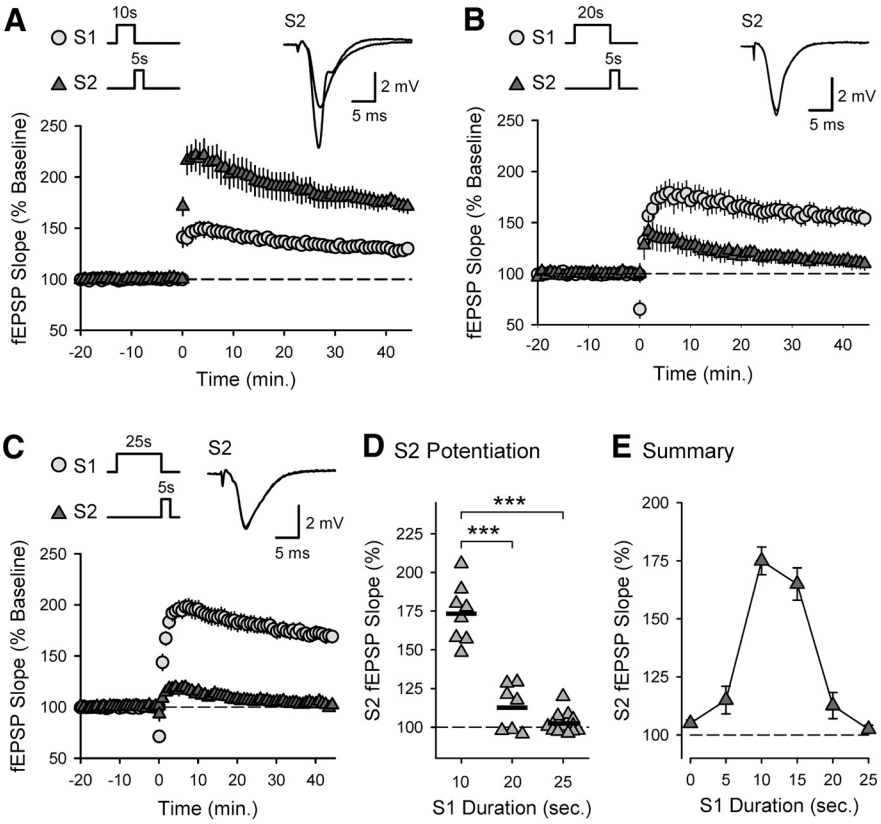

Figure 7. An activity-dependent form of synaptic competition disrupts cooperativity in CS burst-dependent LTP. ***A***, Ten seconds of TPS delivered to S1 synapses (at time = 0) facilitates the induction of LTP by a 5-s-long train of TPS delivered to S2 synapses ($n = 8$). ***B***, ***C***, Increasing the duration of S1 TPS trains to 20 (***B***, $n = 7$) or 25 s (***C***, $n = 13$) fails to enhance LTP induction at S2 synapses. ***A-C***, Traces represent superimposed S2 fEPSPs recorded during baseline and 45 min after S2 TPS. ***D***, Scatter plot represents change in S2 fEPSP slopes (45 min after S2 TPS) from individual experiments. Bars indicate mean values. ***$p < 0.001$, one-way ANOVA with Bonferroni t test *post hoc* comparisons ($F_{(2,25)} = 76.076$, $p < 0.001$). ***E***, Summary plot showing the effect of S1 TPS train duration on the induction of LTP by a 5-s-long train of TPS delivered to S2 synapses. Points include results from experiments shown in Figures 4 and 5 and control experiments in Figure 6*D*.

Although longer trains of TPS delivered to S1 synapses failed to enhance LTP induction at S2 synapses, the facilitation of EPSP-evoked CS bursting at S2 synapses induced by a train of S1 TPS lasting 20 s ($P_{CSB} = 0.995$) (Fig. 8*B*) was not significantly different from that seen in control experiments ($P_{CSB} = 0.945$) (Fig. 8*A*). Twenty-five seconds of TPS delivered to S1 synapses also enhanced EPSP-evoked CS bursting at S2 synapses, although the number of EPSPs evoking CS bursts during 5 s of TPS at S2 synapses ($P_{CSB} = 0.606$) was somewhat reduced compared with control ($p < 0.05$) (Fig. 8*C*). Given the strong dependence of TPS-induced LTP on EPSP-evoked CS bursting (Fig. 2*D*), the failure of S2 synapses to potentiate when S2 TPS is delivered after longer trains of S1 TPS is surprising. However, long trains of TPS induce a pronounced, short-term heterosynaptic depression (Fig. 3*D*) and the heterosynaptic depression induced by S1 TPS trains lasting ≥20 s strongly inhibited TPS-evoked fEPSPs at S2 synapses (Fig. 8*B–D*). Moreover, a comparison of the effect of S1 TPS train duration on CS bursting, LTP induction, and heterosynaptic depression at S2 synapses indicates that LTP induction at S2 synapses wanes as the magnitude of heterosynaptic depression induced by S1 TPS grows (Fig. 8*E*). Notably, the heterosynaptic depression of S2 synapses induced by 25 s of S1 TPS was also associated with a significant reduction in the amplitudes of EPSP-evoked PSs recorded in stratum pyramidale during S2 TPS (Fig. 9). Together, these results suggest that short-term heterosynaptic depression produces a form of synaptic competition that strongly limits cooperative interactions between synapses during the induction of CS burst-dependent LTP.

Strikingly, because of the competition between synapses that develops during longer trains of TPS, CS burst-dependent LTP exhibits properties reminiscent of some forms of cue competition in associative learning. For example, both S1 and S2 synapses potentiated when a total of 30 s of TPS was equally distributed across S1 and S2 synapses (15 s each) (Fig. 10*A*). However, S1 synapses potentiated and S2 synapses failed to undergo LTP when the pattern of S1/S2 synapse activation during a 30-s-long bout of TPS was shifted to more strongly activate S1 synapses (20 s delivered to S1, 10 s delivered to S2; Fig. 10*B*). Consistent with the notion that the stronger activation of S1 synapses enables them to outcompete and prevent LTP induction at S2 synapses, 10 s of TPS did induce LTP at S2 synapses when the duration of S1 TPS was reduced to 10 s to again deliver an equal amount TPS to both sets of synapses (Fig. 10*C*). Although both 10- and 20-s-long trains of TPS delivered to S1 synapses facilitated EPSP-evoked CS bursting at S2 synapses (Fig. 10*D*), 20 s of S1 TPS induced significantly stronger heterosynaptic depression of TPS-evoked fEPSPs at S2 synapses (Fig. 10*E*). Thus, competitive interactions between synapses that develop during longer trains of TPS, perhaps mediated by short-term heterosynaptic depression, produce a form of overshadowing that allows strongly activated synapses to inhibit cooperativity and block LTP induction at more weakly activated synapses.

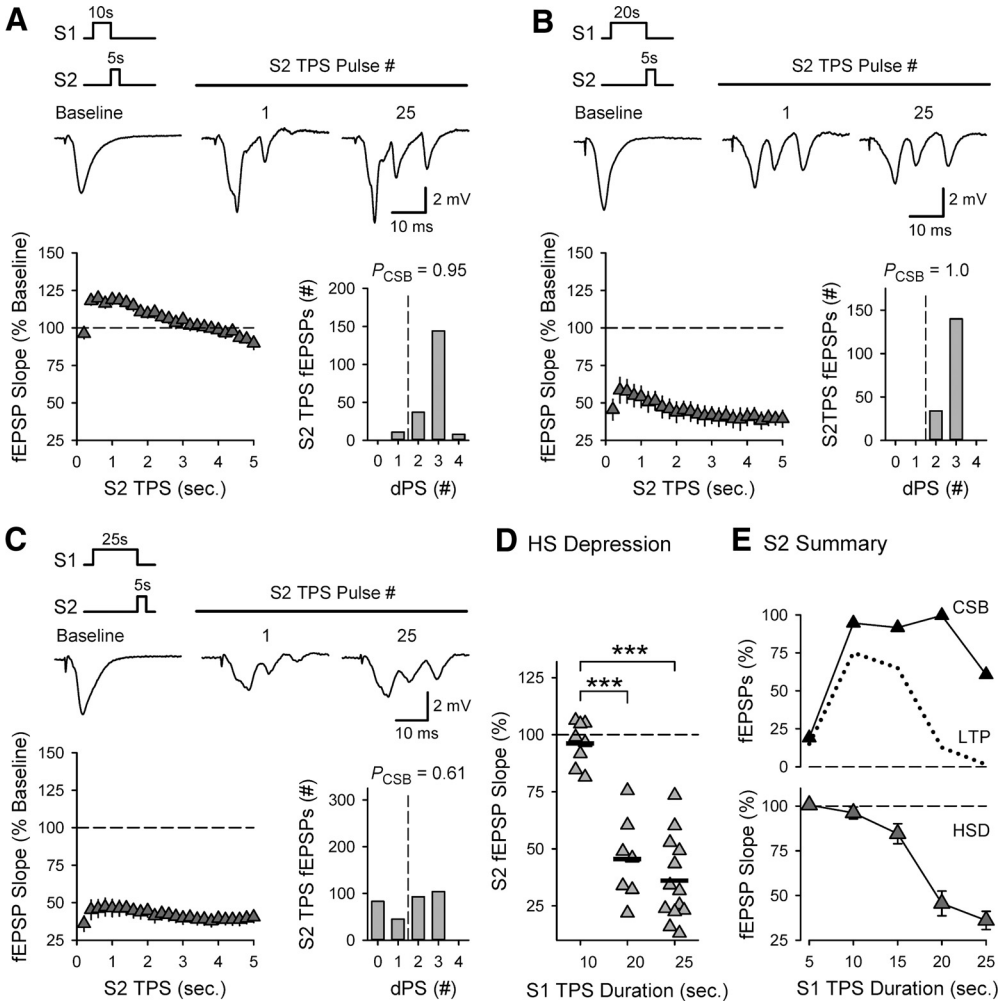

Figure 8. TPS delivered to S1 synapses induces an activity-dependent, heterosynaptic depression that suppresses TPS-evoked EPSPs at S2 synapses. ***A-C***, Left, Plots represent fEPSP slopes (% of pre-S1 TPS baseline) during 5 s of TPS delivered to S2 synapses after 10 (***A***), 20 (***B***), or 25 s (***C***) of TPS delivered to S1 synapses. Traces represent S2 fEPSPs evoked during baseline (before S1 TPS) and during S2 TPS. Right, Histograms represent the number of EPSPs evoking 0-4 dendritic PSs during S2 TPS from all experiments. Results are from the same experiments shown in Figure 7. Although the P_{CSB} during S2 TPS delivered after 20 s of S1 TPS was not significantly different from control (10 s of S1 TPS), P_{CSB} during S2 TPS was significantly reduced when S2 TPS was delivered after 25 s of S1 TPS ($p < 0.05$, one-way ANOVA on ranks with Dunn's test *post hoc* comparisons, $H_{(2)} = 10.473$, $p = 0.005$). ***D***, Heterosynaptic (HS) depression at S2 synapses following TPS delivered to S1 synapses. Points represent slope of first fEPSPs evoked during S2 TPS from all experiments. Bars indicate mean. fEPSPs evoked by the first pulse of S2 TPS were 96 ± 3%, 45 ± 7%, and 36 ± 5% of baseline when S2 TPS was delivered after S1 TPS trains lasting 10, 20, and 25 s, respectively. ***$p < 0.001$, one-way ANOVA with Bonferroni *t* test *post hoc* comparisons ($F_{(2,25)} = 35.171$, $p < 0.001$). ***E***, Bottom, Magnitude of heterosynaptic depression (HSD) at S2 synapses induced by different duration trains TPS delivered to S1 synapses. Top, Effect of S1 TPS train duration on CS bursting (CSB, % of all S2 TPS EPSPs) and LTP induction (% increase from baseline) at S2 synapses is shown for comparison. Points include results from experiments shown in Figures 4 and 5.

CS burst-dependent LTP exhibits a retroactive, non-Hebbian form of cooperativity

As shown in Figure 11*A*, two, brief trains of TPS (5 s duration) delivered to S1 synapses with an ITI of 5 s failed to induce robust CS bursting and had little lasting effect on synaptic transmission. Interestingly, the activity dependence of TPS-induced CS bursting (Fig. 2*A*) predicts that filling the gap between bouts of S1 TPS with a train of TPS delivered to S2 synapses should provide the additional activity needed to shift pyramidal cells into CS bursting mode of AP generation. If so, activation of S2 synapses during the interval between S1 TPS trains should facilitate EPSP-evoked CS bursting during the second train of TPS delivered to S1 synapses and promote LTP at S1 synapses. Consistent with this prediction, although 5 s of TPS delivered to S2 synapses alone had no lasting effect on synaptic strength (Fig. 11*B*), activation of S2 synapses during the interval between trains of TPS delivered to S1 synapses strongly facilitated EPSP-evoked CS bursting and LTP induction at S1 synapses (Fig. 11*C*). Surprisingly, this pattern of TPS also induced LTP at S2 synapses (Fig. 11*C*). Importantly, sequential activation of S1 and S2 synapses with two, 5-s-long trains of TPS (S1 → S2) had little lasting effect on synaptic strength at S2 synapses (Figs. 5*A* and 11*D*). This suggests that the potentiation of S2 synapses induced by this three-train TPS protocol (S1 → S2 → S1) is because of the CS bursting evoked during the final train of TPS delivered to S1 synapses. Thus, CS burst-dependent LTP exhibits a retroactive, non-Hebbian form of cooperativity where, for some patterns of synaptic activity, CS bursts evoked by one set of synapses can trigger LTP induction at other synapses that were active before, but not during, a bout of postsynaptic CS bursting. This suggests that the S1 → S2 → S1 pattern of TPS used in these experiments sets an eligibility trace at S2 synapses that is updated by the subsequent bout of postsynaptic CS bursting evoked during the final train TPS delivered to S1 synapses.

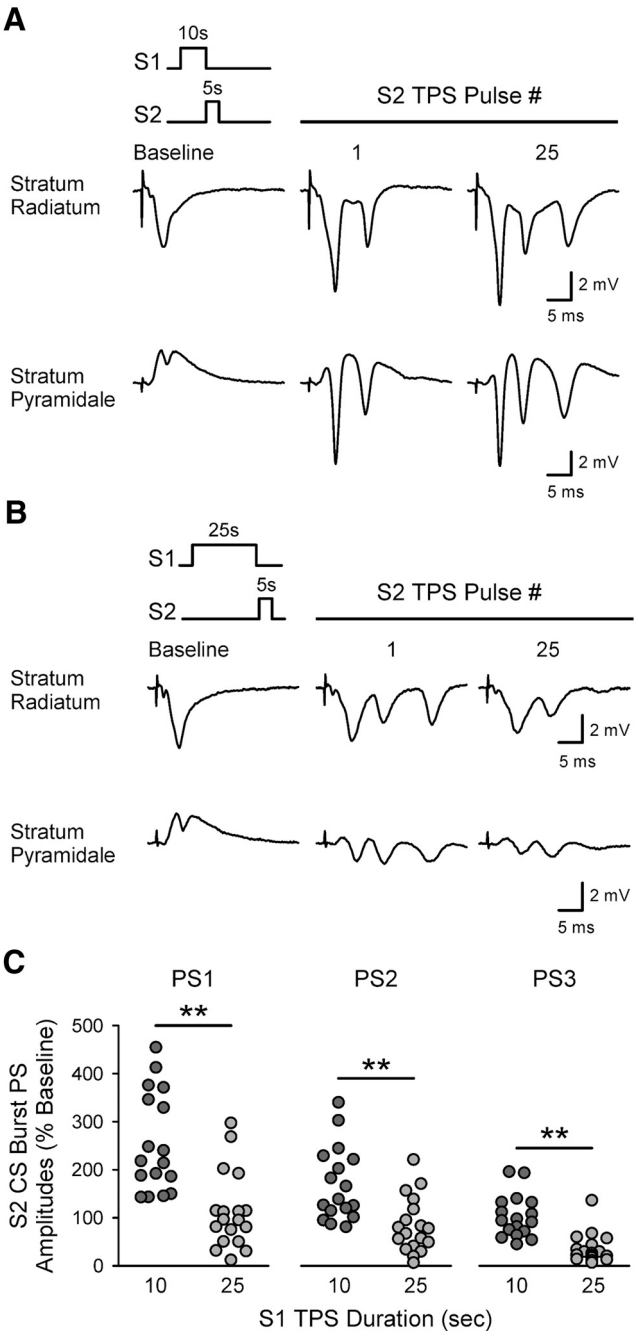

Figure 9. Heterosynaptic inhibition of CS burst PS amplitudes. ***A***, ***B***, Traces represent postsynaptic responses simultaneously recorded in stratum radiatum and stratum pyramidale during 5 s of TPS delivered to S2 synapses after either 10 (***A***) or 25 s (***B***) of TPS delivered to S1 synapses. ***C***, Scatter plots represent mean amplitudes of first, second, and third PSs of CS bursts elicited during S2 TPS from individual experiments where S2 TPS was delivered after 10 ($n = 17$) or 25 s of S1 TPS ($n = 18$). $^{**}p < 0.001$ (Mann–Whitney rank-sum comparisons, $U = 36$, 48, and 23 for first, second and third PSs, respectively).

Previous findings indicate that eligibility traces set by spike timing-dependent plasticity stimulation protocols (He et al., 2015; Fisher et al., 2017; Shindou et al., 2019) or a brief bout of 20 Hz presynaptic fiber stimulation (Bittner et al., 2017) decay over a few seconds. Thus, to determine the time course of TPS-induced eligibility traces, I next examined how synaptic strength at S2 synapses is altered by three-train TPS protocols (S1 → S2 → S1) where the final train of TPS was delivered to S1 synapses with a delay of 2-8 s after S2 TPS (Fig. 12). When the final train of TPS was delivered to S1 synapses 2 s after activation of S2 synapses, S1 EPSPs evoked strong CS bursting and both S1 and S2 synapses potentiated (Fig. 12*A*). S2 (and S1) synapses also potentiated when the final train of S1 TPS was delayed by 4 s (Fig. 12*B*). However, CS bursting at S1 synapses, and LTP induction at both S1 and S2 synapses, were reduced when the final train of TPS was delivered 8 s after activation of S2 synapses (Fig. 12*C*). Thus, TPS-induced eligibility traces persist for at least 4 s (Fig. 12*D*). As expected from the results shown in Figure 6, the heterosynaptic facilitation of LTP induction at S1 synapses produced by activation of S2 synapses during the interval between S1 TPS trains exhibited a similar time course (Fig. 12*D*). Thus, while TPS delivered to S2 synapses facilitates EPSP-evoked CS bursting and LTP induction at S1 synapses, activation of S1 synapses with a brief train of TPS, in turn, triggers eligibility trace update and potentiation at S2 synapses. This indicates that cooperativity in CS burst-dependent LTP arises from highly synergistic, proactive and retroactive interactions between asynchronously activated synapses occurring over behaviorally relevant timescales of several seconds. Notably, high-frequency trains of single spikes evoked by HFS delivered to S1 synapses failed to update eligibility traces at S2 synapses (Fig. 13), suggesting that postsynaptic CS bursting provides a unique, instructive signal for adjusting synaptic strength through eligibility trace update.

Discussion

Although conventional Hebbian LTP and CS burst-dependent LTP share a number of properties expected of synaptic mechanisms involved in associative learning, CS burst-dependent LTP exhibits two important properties not seen in conventional Hebbian LTP. First, cooperative, and thus associative, interactions between synapses in Hebbian LTP are restricted to millisecond timescales, whereas CS burst-dependent LTP exhibits an unusual, temporally bidirectional form of cooperativity that operates on behavioral timescales of several seconds. Second, unlike standard Hebbian LTP, CS burst-dependent LTP is potently regulated by activity-dependent, competitive interactions between synapses.

Although a number of potential mechanisms could contribute to behavioral timescale cooperativity in CS burst-dependent LTP, the ability of TPS protocols to induce a short-term, heterosynaptic facilitation of EPSP-evoked CS bursting likely has a key role. As shown in Figure 6, TPS induces a short-term, heterosynaptic facilitation of EPSP-evoked CS bursting that persists for several seconds, thereby generating a relatively broad temporal interval during which multiple, asynchronously active synaptic inputs can interact in a cooperative manner to undergo LTP. Interestingly, the short-term facilitation of CS bursting that follows TPS allows CS burst-dependent LTP to retain the correlative properties of Hebbian plasticity (i.e., synapses potentiate in response to coincident presynaptic activity and postsynaptic CS bursting), while at the same time expanding the cooperative and associative properties of LTP induction to timescales that can support associative learning. Although the mechanisms responsible for short-term facilitation of CS burst firing following a bout of TPS are unknown, GABAergic inhibition, synaptic SK-type K^+ channels, and dendritic A-type K^+ channels all potently suppress CS bursting in CA1 pyramidal cells (Magee and Carruth, 1999; Babiec et al., 2017). Thus, a short-term depression of inhibitory synaptic transmission (Davies et al., 1991; Mott and Lewis, 1991) and/or an activity-dependent inhibition of SK (Lin et al., 2008) or A-type K^+ channels (Winder et al., 1999; Morozov et

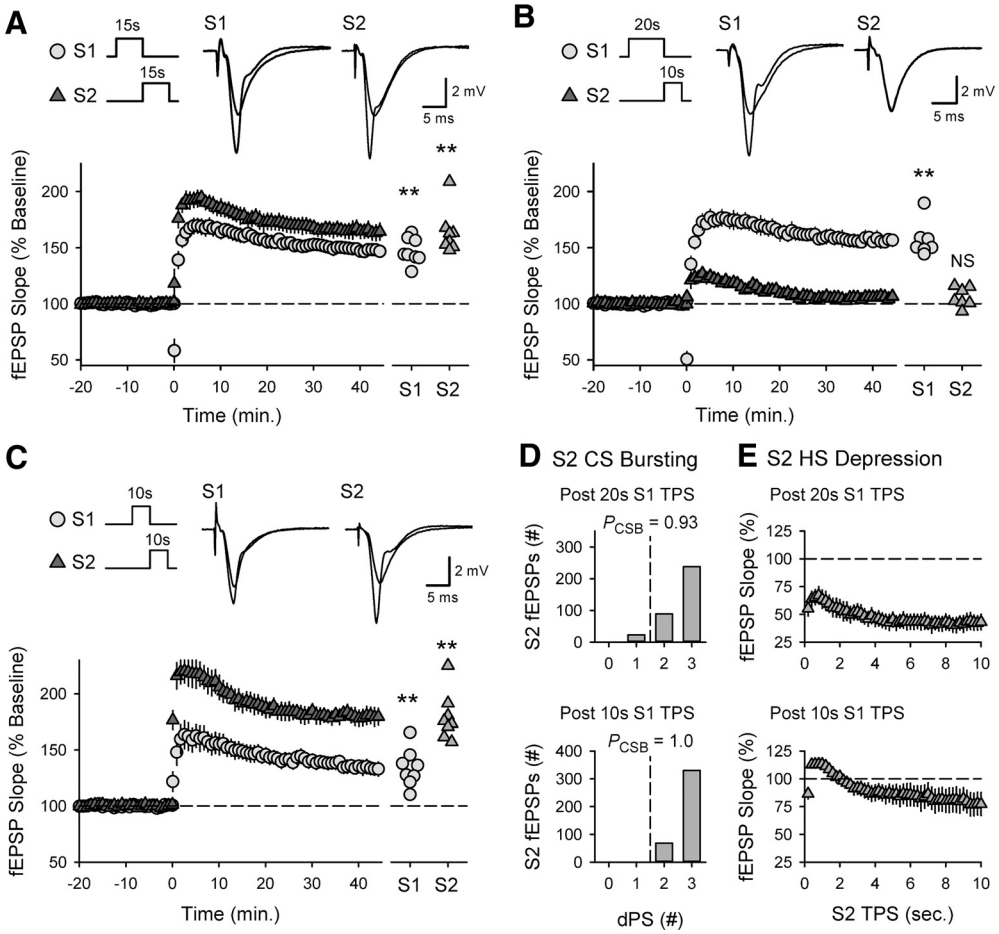

Figure 10. Strongly activated synapses block CS burst-dependent LTP induction at more weakly activated synapses. ***A***, Thirty seconds of TPS, equally divided between S1 and S2 synapses (S1 TPS before S2 TPS), was delivered at time = 0. At 45 min after TPS, S1 fEPSPs were 147 ± 4% of baseline and S2 fEPSPs were 164 ± 7% of baseline ($n = 8$). Scatter plot represents fEPSP slopes 45 min after TPS from all experiments. $^{**}p < 0.001$, paired t test comparisons with pre-TPS baseline (S1: $t_{(7)} = 8.919$, $p = 4.52 \times 10^{-5}$, S2: $t_{(7)} = 12.123$, $p = 5.94 \times 10^{-6}$). ***B***, Twenty seconds of TPS was delivered to S1 synapses before 10 s of TPS delivered to S2 synapses. At 45 min after TPS, S1 fEPSPs were 157 ± 6% of baseline and S2 fEPSPs were 106 ± 3% of baseline ($n = 7$). $^{**}p < 0.001$, paired t test comparisons with pre-TPS baseline (S1: $t_{(6)} = 9.523$, $p = 7.65 \times 10^{-5}$, S2: $t_{(6)} = 1.793$, $p = 0.123$). ***C***, Same as in ***B***, but with S1 TPS reduced to 10 s. At 45 min after TPS, S1 fEPSPs were 134 ± 6% of baseline and S2 fEPSPs were 179 ± 8% of baseline ($n = 8$). $^{**}p < 0.001$, paired t test comparison with baseline (S1: $t_{(7)} = 6.063$, $p = 5.09 \times 10^{-4}$, S2: $t_{(7)} = 10.594$, $p = 1.46 \times 10^{-5}$). ***A-C***, Traces represent superimposed fEPSPs recorded during baseline and 45 min after TPS. ***D***, Histograms represent the number of EPSPs evoking 0-3 PSs during 10 s of S2 TPS delivered after 20 (top) or 10 s (bottom) of S1 TPS from all experiments. ***E***, Heterosynaptic (HS) depression of S2 fEPSPs by prior activation of S1 synapses. Plots represent slopes of fEPSPs evoked during TPS at S2 synapses delivered after 20 (top) or 10 s (bottom) of TPS delivered to S1 synapses. At the start of TPS, S2 fEPSPs were reduced to 55 ± 7% of baseline following 20 s of S1 TPS and were 86 ± 5% of baseline following 10 s of S1 TPS ($t_{(13)} = 3.874$, $p = 0.00192$). ***D***, ***E***, Results are from the same experiments shown in ***B***, ***C***.

al., 2003) may enable a transient facilitation of EPSP-evoked CS bursting following TPS.

Results from experiments using triplet patterns of TPS (Figs. 11 and 12) suggest that cooperativity in CS burst-dependent LTP is also mediated by a non-Hebbian form of plasticity that enables LTP induction at synapses that were active before, but not during, a bout of postsynaptic CS bursting. One explanation for this unusual, retroactive form of cooperativity is that the S1 → S2 pattern of TPS used in these experiments sets an eligibility trace at S2 synapses that enables potentiation in response to a delayed bout of CS bursting triggered by other synaptic inputs. Consistent with this notion, the potentiation of S2 synapses by S1 → S2 → S1 TPS protocols is similar to behavioral timescale synaptic plasticity, where a non-Hebbian updating of synaptic eligibility traces by dendritic plateau potentials generates place-specific firing in CA1 pyramidal cells (Bittner et al., 2017). The molecular mechanisms responsible for synaptic eligibility traces, and how they enable LTP induction by noncontingent postsynaptic CS bursting, are important questions for future studies. It is interesting, however, that bouts of high-frequency synaptic stimulation are unable to update TPS-induced eligibility traces (Fig. 13). This suggests that CS bursts provide a unique signal for LTP induction through eligibility trace update. Notably, although APs can backpropagate into the apical dendrites of pyramidal cells, the amplitude of backpropagating APs is strongly attenuated with distance from the cell body, especially during bouts of high-frequency single spiking (Spruston et al., 1995; Callaway and Ross, 1995). In contrast, dendritically initiated spikes and plateau potentials, which trigger somatic CS bursting, produce stronger dendritic depolarization and calcium influx compared with backpropagating APs (Golding et al., 2002; Grienberger et al., 2014). Thus, the induction of LTP by eligibility trace update may require the stronger depolarization produced by dendritic spiking. If so, this could provide a mechanism that protects eligibility traces from ongoing, single spike firing and thus prevent spurious changes in synaptic weights by activity related to processing other forms of information.

Although the activity-dependent competitive interactions between synapses that develop during TPS are striking, understanding the functional significance of synaptic competition in

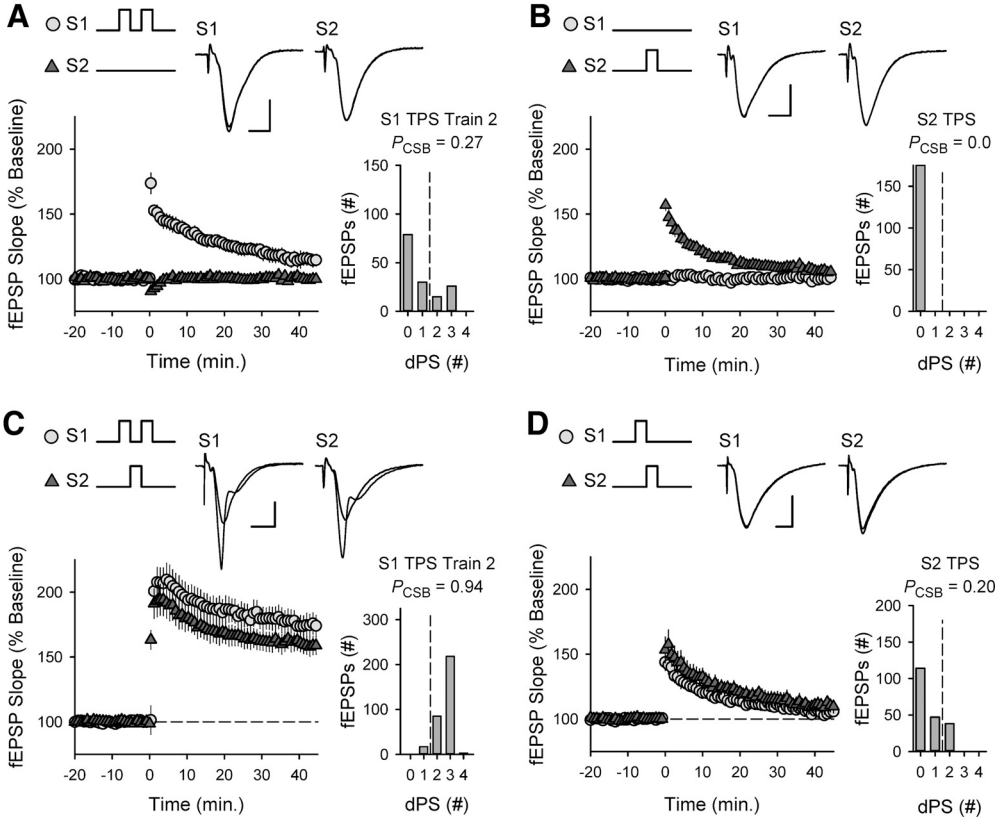

Figure 11. CS burst-dependent LTP exhibits a retroactive, non-Hebbian form of cooperativity. ***A***, Two trains of TPS (both 5 s in duration, ITI = 5 s) were delivered to S1 synapses (at time = 0). At 45 min after TPS stimulation, S1 fEPSPs were 115 ± 5% of baseline, $n = 6$. ***B***, A single train of TPS (duration = 5s) was delivered (at time = 0) to S2 synapses. At 45 min after TPS, S2 fEPSPs were 103 ± 3% of baseline, $n = 7$. ***C***, Triplet pattern of TPS (S1 → S2 → S1) where activation of S2 synapses fills the ITI between S1 TPS trains was delivered at time = 0. At 45 min following triplet TPS stimulation, S1 fEPSPs were potentiated to 175 ± 8% of baseline and S2 fEPSPs were potentiated to 159 ± 7% of baseline, $n = 13$. ***D***, Sequential trains of TPS (S1 → S2, each 5 s long) were delivered to S1 and S2 synapses at time = 0. At 45 min after TPS, S1 and S2 fEPSPs were 105 ± 3% and 111 ± 5% of baseline, respectively ($n = 8$). ***A-D***, Histograms represent the number of EPSPs eliciting 0-4 dendritic PSs during the indicated trains of TPS from all experiments. The P_{CSB} during the second train of TPS delivered to S1 synapses was significantly enhanced when TPS was delivered to S2 synapses during the interval between S1 TPS trains (Mann–Whitney $U = 3.5$, $p = 0.001$). ***A-D***, Traces represent superimposed fEPSPs elicited by S1 and S2 stimulation recorded during baseline and 45 min after TPS.

CS burst-dependent LTP will require further investigation. One possibility is that synaptic competition serves as a form of homeostatic plasticity that prevents excessive, runaway LTP induction during prolonged bouts of postsynaptic CS bursting. Indeed, the properties of synaptic competition in CS burst-dependent LTP are consistent with key features of synaptic competition in the Bienenstock, Cooper, and Munro (BCM) plasticity rule (Bienenstock et al., 1982). In the BCM model, activity-dependent changes in synaptic strength are regulated in a cell-wide manner by a modification threshold, θ_M, where synapses that drive frequencies of postsynaptic spiking greater than θ_M undergo LTP. Importantly, θ_M is dynamically regulated as a function of postsynaptic firing such that the ability of all synapses onto a postsynaptic cell to undergo LTP is reduced after a bout of high-frequency postsynaptic spiking. Thus, the synaptic competition induced by longer bouts of postsynaptic CS bursting provides a mechanism to implement the activity-dependent and heterosynaptic shift in θ_M that underlies competitive synaptic interactions in the BCM model. Another intriguing feature of synapse competition in CS burst-dependent LTP is its relatively fast mode of operation. Notably, although cortical synapses exhibit experience-dependent shifts in θ_M following sensory deprivation, these changes develop very slowly (over 24 h or more) (Kirkwood et al., 1996; Hardingham et al., 2008). Importantly, computational models indicate that this is far too slow to stabilize activity-dependent changes in synaptic strength (Toyoizumi et al., 2014) and protect neuronal networks from runaway activity associated with Hebbian LTP (Zenke et al., 2013). In contrast, the induction of CS burst-dependent LTP and the onset of synapse competition during TPS operate on similar timescales. Thus, the relatively rapid onset of synaptic competition in CS burst-dependent LTP is consistent with results from computational studies indicating that stable activity in neural networks with Hebbian synapses requires rapid, negative feedback mechanisms to control LTP induction (Zenke et al., 2017; Zenke and Gerstner, 2017).

The observation that the loss of cooperative LTP induction coincides with the onset of heterosynaptic depression (Fig. 8*E*) suggests an important role for short-term heterosynaptic depression in constraining CS burst-dependent LTP. Consistent with this notion, short-term heterosynaptic depression at excitatory synapses onto CA1 pyramidal cells is because of a presynaptic inhibition of transmitter release (Isaacson et al., 1993; Grover and Teyler, 1993; Manzoni et al., 1994). Thus, the heterosynaptic depression induced by TPS may suppress LTP induction at other synapses by inhibiting glutamate release and reducing postsynaptic bursting, thereby limiting activation of postsynaptic NMDARs. Interestingly, short-term heterosynaptic depression at excitatory synapses onto CA1 pyramidal cells is mediated by activation of presynaptic, A1-type adenosine

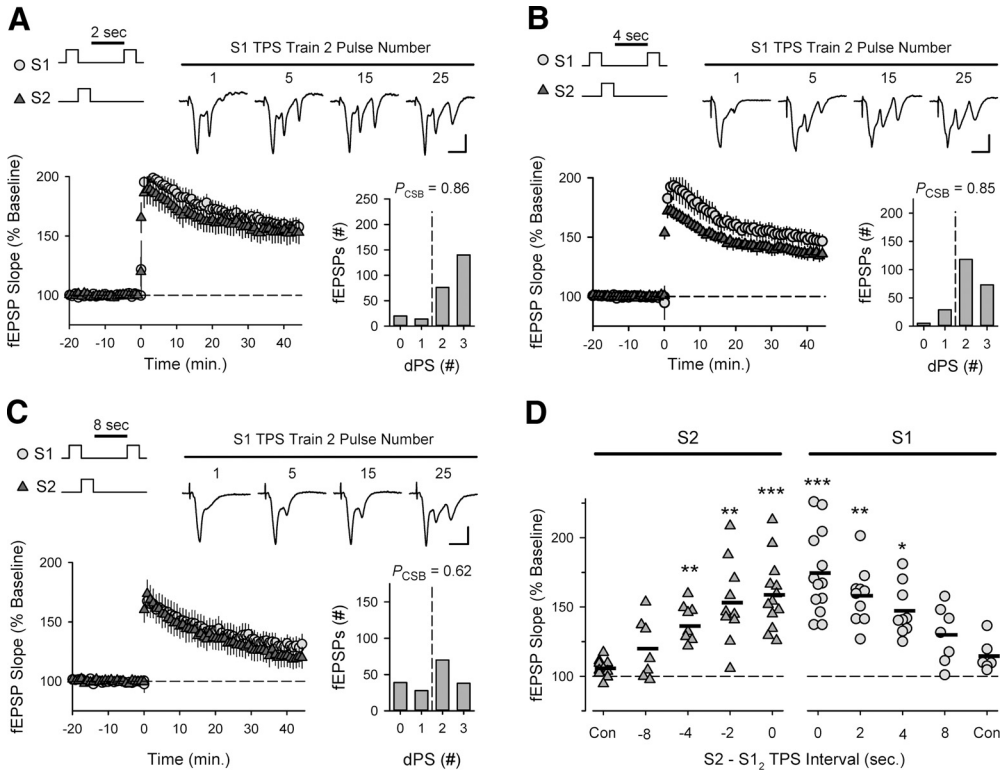

Figure 12. Time course of retroactive non-Hebbian cooperativity in CS burst-dependent LTP. ***A-C***, Following S1 → S2 trains of TPS (each 5 s in duration), a third train of TPS was delivered to S1 synapses with a delay of 2 (***A***, $n = 10$), 4 (***B***, $n = 9$), or 8 s (***C***, $n = 7$). Histograms represent the number of fEPSPs eliciting 0-3 dendritic PSs during the final TPS train delivered to S1 synapses from all experiments. Traces represent fEPSPs elicited at the indicated stimulation pulse numbers during the final S1 TPS train. Calibration: 2 mV, 10 ms. ***D***, Summary plot showing the effect of the ITI between second and third trains of TPS on LTP induction. Symbols represent change in fEPSP slopes (45 min after last TPS train) from individual experiments. Bars indicate mean values. S1 controls (con) are from experiments shown in Figure 11*A*. S2 controls are from experiments shown in Figure 11*B*. Points for ITIs = 0 are from experiments shown in Figure 11*C*. ***$p < 0.001$; **$p < 0.01$; *$p < 0.05$; compared with S1 or S2 controls, one-way ANOVA with Bonferroni *t* test *post hoc* comparisons (S1: $F_{(4,40)} = 9.095$, $p < 0.001$; S2: $F_{(4,44)} = 10.974$, $p < 0.001$).

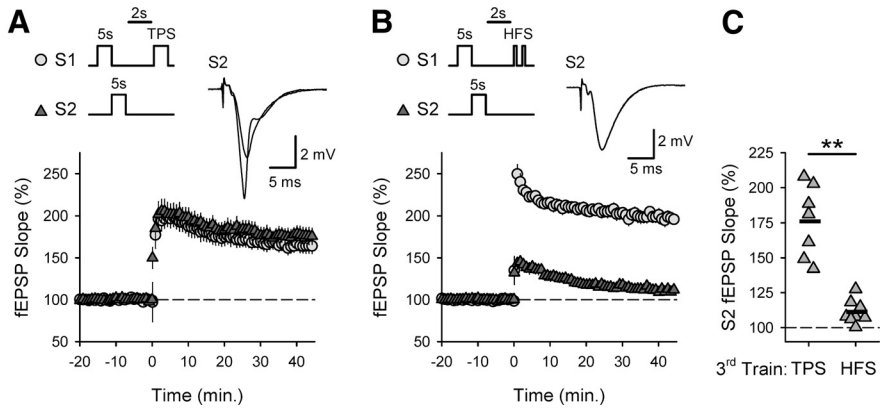

Figure 13. High-frequency trains of single spikes fail to update TPS-induced eligibility traces. ***A***, Following two sequential, 5-s-long trains of TPS delivered to S1 and S2 synapses, a third train of TPS delivered to S1 synapses (duration = 5 s, ITI = 2 s) induces LTP at both S1 and S2 synapses ($n = 7$). ***B***, HFS of S1 synapses delivered 2 s after sequential trains of TPS-5s delivered to S1 and S2 synapses fails to induce LTP at S2 synapses ($n = 8$). Traces represent superimposed S2 fEPSPs recorded during baseline and 45 min after the final train of TPS or HFS delivered to S1 synapses. ***C***, Summary plot showing change in S2 fEPSP slopes when the third train in the stimulation protocol was either TPS or HFS delivered to S1 synapses. Symbols are results from individual experiments. Bars indicate mean values. At 45 min after the final S1 stimulation train, S2 synapses were potentiated to 176 ± 10% of baseline when TPS was delivered to S1 synapses and were 111 ± 3% of baseline when HFS was delivered to S1 synapses ($t_{(13)} = 6.727$, $^{**}p = 1.41 \times 10^{-5}$).

receptors following adenosine release from pyramidal cells in response to postsynaptic APs (Lovatt et al., 2012; Wall and Dale, 2013). Thus, during prolonged bouts of postsynaptic CS bursting, adenosine released from CA1 pyramidal cells may act as a retrograde transmitter that produces a widespread inhibition of LTP induction by suppressing glutamate release at excitatory synapses. There are, however, alternative mechanisms, such as ATP release from astrocytes (Serrano et al., 2006; Boddum et al., 2016) or activity-dependent inhibition of presynaptic function via endocannabinoid signaling (Kreitzer and Regehr, 2001; Ohno-Shosaku et al., 2002), that could mediate synaptic competition in CS burst-dependent LTP. Moreover, very long trains of TPS (3 min) induce a heterosynaptic inhibition of protein synthesis-dependent LTP induced by HFS protocols (Young and Nguyen, 2005). Thus, postsynaptic forms of meta-plasticity could contribute as well (Abraham, 2008).

Despite many decades of research, the notion that Hebbian forms of plasticity underlie learning and memory formation remains controversial (Gallistel and Matzel, 2013; Bannerman et al., 2014; Grant, 2018). Emerging evidence suggests, however, that Hebbian plasticity is just one component of a larger collection of NMDAR-dependent plasticity rules that can regulate activity-dependent increases in synaptic strength

during learning (Gerstner et al., 2018; Magee and Grienberger, 2020). Consistent with this notion, CS burst-dependent LTP exhibits a number of intriguing properties that can overcome significant limitations of conventional Hebbian plasticity. Thus, a better understanding of the properties, and underlying mechanisms, of CS burst-dependent LTP should provide important insights into the synaptic mechanisms of learning and memory formation.

References

Abraham WC (2008) Metaplasticity: tuning synapses and networks for plasticity. Nat Rev Neurosci 9:387–399.

Azouz R, Jensen MS, Yaari Y (1996) Ionic basis of spike after-depolarization and burst generation in adult rat hippocampal CA1 pyramidal cells. J Physiol 492:211–223.

Babiec WE, Jami SA, Guglietta R, Chen PB, O'Dell TJ (2017) Differential regulation of NMDA receptor-mediated transmission by SK channels underlies dorsal-ventral differences in dynamics of Schaffer collateral synaptic function. J Neurosci 37:1950–1964.

Bannerman DM, Sprengel R, Sanderson DJ, McHugh SB, Rawlins JN, Monyer H, Seeburg PH (2014) Hippocampal synaptic plasticity, spatial memory and anxiety. Nat Rev Neurosci 15:181–192.

Barrionuevo G, Brown TH (1983) Associative long-term potentiation in hippocampal slices. Proc Natl Acad Sci USA 80:7347–7351.

Bienenstock EL, Cooper LN, Munro PW (1982) Theory for the development of neuron selectivity: orientation specificity and binocular interaction in visual cortex. J Neurosci 2:32–48.

Bittner KC, Milstein AD, Grienberger C, Romani S, Magee JC (2017) Behavioral timescale synaptic plasticity underlies CA1 place fields. Science 357:1033–1036.

Boddum K, Jensen TP, Magloire V, Kristiansen U, Rusakov DA, Pavlov I, Walker MC (2016) Astrocytic GABA transporter activity modulates excitatory neurotransmission. Nat Commun 7:13572.

Brown GP, Blitzer RD, Connor JH, Wong T, Shenolikar S, Iyengar R, Landau EM (2000) Long-term potentiation induced by theta frequency stimulation is regulated by a protein phosphatase-1-operated gate. J Neurosci 20:7880–7887.

Brzosko Z, Mierau SB, Paulsen O (2019) Neuromodulation of spike-timing-dependent plasticity: past, present, and future. Neuron 103:563–581.

Callaway JC, Ross WN (1995) Frequency-dependent propagation of sodium action potentials in dendrites of hippocampal CA1 pyramidal neurons. J Neurophysiol 74:1395–1403.

Davies CH, Starkey SJ, Pozza MF, Collingridge GL (1991) GABA auto-receptors regulate the induction of LTP. Nature 349:609–611.

Debanne D, Gähwiler BH, Thompson SM (1996) Cooperative interactions in the induction of long-term potentiation and depression of synaptic excitation between hippocampal CA3-CA1 pairs in vitro. Proc Natl Acad Sci USA 93:11225–11230.

Dringenberg HC (2020) The history of long-term potentiation as a memory mechanism: controversies, confirmation, and some lessons to remember. Hippocampus 30:987–1012.

Epsztein J, Brecht M, Lee AK (2011) Intracellular determinants of hippocampal CA1 place and silent cell activity in a novel environment. Neuron 70:109–120.

Fanselow MS, Wassum KM (2016) The origins and organization of vertebrate Pavlovian conditioning. Cold Spring Harb Perspect Biol 8:a021717.

Fink AE, O'Dell TJ (2009) Short trains of theta frequency stimulation enhance CA1 pyramidal neuron excitability in the absence of synaptic potentiation. J Neurosci 29:11203–11214.

Fisher SD, Robertson PB, Black MJ, Redgrave P, Sagar MA, Abraham WC, Reynolds JNJ (2017) Reinforcement determines the timing dependence of corticostriatal synaptic plasticity in vivo. Nat Commun 8:334.

Gallistel CR, Matzel LD (2013) The neuroscience of learning: beyond the Hebbian synapse. Annu Rev Psychol 64:169–200.

Gerstner W, Lehmann M, Liakoni V, Corneil D, Brea J (2018) Eligibility traces and plasticity on behavioral timescales: experimental support of neoHebbian three-factor learning Rules. Front Neural Circuits 12:53.

Golding NL, Staff NP, Spruston N (2002) Dendritic spikes as a mechanism for cooperative long-term potentiation. Nature 418:326–331.

Grant SG (2018) Synapse molecular complexity and the plasticity behavior problem. Brain Neurosci Adv. Doi: 10.1177/2398212818810685.

Grienberger C, Chen X, Konnerth A (2014) NMDA receptor-dependent multidendrite Ca^{2+} spikes required for hippocampal burst firing in vivo. Neuron 81:1274–1281.

Grover LM, Teyler TJ (1993) Presynaptic mechanism for heterosynaptic, posttetanic depression in area CA1 of rat hippocampus. Synapse 15:149–157.

Gustafsson B, Wigström H (1986) Hippocampal long-lasting potentiation produced by pairing single volleys and brief conditioning tetani evoked in separate afferents. J Neurosci 6:1575–1582.

Hardingham N, Wright N, Dachtler J, Fox K (2008) Sensory deprivation unmasks a PKA-dependent synaptic plasticity mechanism that operates in parallel with CaMKII. Neuron 60:861–874.

Harris KD, Hirase H, Leinekugel X, Henze DA, Buzsáki G (2001) Temporal interaction between single spikes and complex spike bursts in hippocampal pyramidal cells. Neuron 32:141–149.

He K, Huertas M, Hong SZ, Tie XX, Hell JW, Shouval H, Kirkwood A (2015) Distinct eligibility traces for LTP and LTD in cortical synapses. Neuron 88:528–538.

Isaacson JS, Solis JM, Nicoll RA (1993) Local and diffuse synaptic actions of GABA in the hippocampus. Neuron 10:165–175.

Izhikevich EM (2007) Solving the distal reward problem through linkage of STDP and dopamine signaling. Cereb Cortex 17:2443–2452.

Kamin LJ (1969) Predictability, surprise, attention, and conditioning. In: Punishment and aversive behavior (Campbell BS, Church RM, eds), pp 279–296. New York: Appleton-Century-Crofts.

Kelso SR, Brown TH (1986) Differential conditioning of associative synaptic enhancement in hippocampal brain slices. Science 232:85–87.

Kelso SR, Ganong AH, Brown TH (1986) Hebbian synapses in hippocampus. Proc Natl Acad Sci USA 83:5326–5330.

Kirkwood A, Rioult MG, Bear MF (1996) Experience-dependent modification of synaptic plasticity in visual cortex. Nature 381:526–528.

Klyachko VA, Stevens CF (2006) Excitatory and feed-forward inhibitory hippocampal synapses work synergistically as an adaptive filter of natural spike trains. PLoS Biol 4:e207.

Kreitzer AC, Regehr WG (2001) Retrograde inhibition of presynaptic calcium influx by endogenous cannabinoids at excitatory synapses onto Purkinje cells. Neuron 29:717–727.

Larkum ME, Zhu JJ, Sakmann B (1999) A new cellular mechanism for coupling inputs arriving at different cortical layers. Nature 398:338–341.

Lee KS (1983) Cooperativity among afferents for the induction of long-term potentiation in the CA1 region of the hippocampus. J Neurosci 3:1369–1372.

Lin MT, Lujan R, Watanabe M, Adelman JP, Maylie J (2008) SK2 channel plasticity contributes to LTP at Schaffer collateral-CA1 synapses. Nat Neurosci 11:170–177.

Lovatt D, Xu Q, Liu W, Takano T, Smith NA, Schnermann J, Tieu K, Nedergaard M (2012) Neuronal adenosine release, and not astrocytic ATP release, mediates feedback inhibition of excitatory activity. Proc Natl Acad Sci USA 109:6265–6270.

Lovett-Barron M, Turi GF, Kaifosh P, Lee PH, Bolze F, Sun XH, Nicoud JF, Zemelman BV, Sternson SM, Losonczy A (2012) Regulation of neuronal input transformation by tunable dendritic inhibition. Nat Neurosci 15:423–430.

Mackintosh NJ (1976) Overshadowing and stimulus intensity. Anim Learn Behav 4:186–192.

Magee JC, Carruth M (1999) Dendritic voltage-gated ion channels regulate the action potential firing mode of hippocampal CA1 pyramidal cell. J Neurophysiol 82:1895–1901.

Magee JC, Grienberger C (2020) Synaptic plasticity forms and functions. Annu Rev Neurosci 43:95–117.

Magee JC, Johnston D (1997) A synaptically controlled, associative signal for Hebbian plasticity in hippocampal neurons. Science 275:209–213.

Manzoni OJ, Manabe T, Nicoll RA (1994) Release of adenosine by activation of NMDA receptors in the hippocampus. Science 265:2098–2101.

McNaughton BL, Douglas RM, Goddard GV (1978) Synaptic enhancement in fascia dentata: cooperativity among coactive afferents. Brain Res 157:277–293.

Morozov A, Muzzio IA, Bourtchouladze R, Van-Strien N, Lapidus K, Yin D, Winder DG, Adams JP, Sweatt JD, Kandel ER (2003) Rap1 couples

cAMP signaling to a distinct pool of p42/44 MAPK regulating excitability, synaptic plasticity, learning, and memory. Neuron 39:309–325.
Mott DD, Lewis DV (1991) Facilitation of the induction of long-term potentiation by $GABA_B$ receptors. Science 252:1718–1720.
Ohno-Shosaku T, Tsubokawa H, Mizushima I, Yoneda N, Zimmer A, Kano M (2002) Presynaptic cannabinoid sensitivity is a major determinant of depolarization-induced retrograde suppression at hippocampal synapse. J Neurosci 22:3864–3872.
Pavlov I (1927) Conditioned reflexes, an investigation of the psychological activity of the cerebral cortex. Oxford: Oxford UP.
Payeur A, Guerguiev J, Zenke F, Richards BA, Naud R (2021) Burst-dependent synaptic plasticity can coordinate learning in hierarchical circuits. Nat Neurosci 24:1010–1019.
Richards BA, Lillicrap TP (2019) Dendritic solutions to the credit assignment problem. Curr Opin Neurobiol 54:28–36.
Royer S, Zemelman BV, Losonczy A, Kim J, Chance F, Magee JC, Buzsáki G (2012) Control of timing, rate and bursts of hippocampal place cells by dendritic and somatic inhibition. Nat Neurosci 15:769–775.
Sastry BR, Goh JW, Auyeung A (1986) Associative induction of posttetanic and long-term potentiation in CA1 neurons of rat hippocampus. Science 232:988–990.
Serrano A, Haddjeri N, Lacaille JC, Robitaille R (2006) GABAergic network activation of glial cells underlies hippocampal heterosynaptic depression. J Neurosci 26:5370–5382.
Shindou T, Shindou M, Watanabe S, Wickens J (2019) A silent eligibility traces enables dopamine-dependent synaptic plasticity for reinforcement learning in the mouse striatum. Eur J Neurosci 49:726–736.
Spruston N, Schiller Y, Stuart G, Sakmann B (1995) Activity-dependent action potential invasion and calcium influx into hippocampal CA1 dendrites. Science 268:297–300.
Stuart GJ, Sakmann B (1994) Active propagation of somatic action potentials into neocortical pyramidal cell dendrites. Nature 367:69–72.
Takahashi H, Magee JC (2009) Pathway interactions and synaptic plasticity in the dendritic tuft regions of CA1 pyramidal neurons. Neuron 62:102–111.
Thomas MJ, Watabe AM, Moody TD, Makhinson M, O'Dell TJ (1998) Postsynaptic complex spike bursting enables the induction of LTP by theta frequency synaptic stimulation. J Neurosci 18:7118–7126.
Tombaugh GC, Rowe WB, Chow AR, Michael TH, Rose GM (2002) Theta-frequency synaptic potentiation in CA1 in vitro distinguishes cognitively impaired from unimpaired aged Fischer 344 rats. J Neurosci 22:9932–9940.
Toyoizumi T, Kaneko M, Stryker MP, Miller KD (2014) Modeling the dynamic interaction of Hebbian and homeostatic plasticity. Neuron 84:497–510.
Wall MJ, Dale N (2013) Neuronal transporter and astrocytic ATP exocytosis underlie activity-dependent adenosine release in the hippocampus. J Physiol 591:3853–3871.
Winder DG, Martin KC, Muzzio IA, Rohrer D, Chruscinski A, Kobilka B, Kandel ER (1999) ERK plays a regulatory role in induction of LTP by theta frequency stimulation and its modulation by β-adrenergic receptors. Neuron 24:715–726.
Young JZ, Nguyen PV (2005) Homosynaptic and inhibition of synaptic tagging and capture of long-term potentiation by previous synaptic activity. J Neurosci 25:7221–7231.
Zenke F, Gerstner W (2017) Hebbian plasticity requires compensatory processes on multiple timescales. Philos Trans R Soc Lond B Biol Sci 372:20160259.
Zenke F, Hennequin G, Gerstner W (2013) Synaptic plasticity in neural networks needs homeostasis with a fast rate detector. PLoS Comput Biol 9: e1003330.
Zenke F, Gerstner W, Ganguli S (2017) The temporal paradox of Hebbian learning and homeostatic plasticity. Curr Opin Neurobiol 43:166–176.